

# Synthesis, Structure, and Reactivity of Chiral Rhenium Cycloalkene Complexes of the Formula

## $[(\eta^5\text{-C}_5\text{H}_5)\text{Re}(\text{NO})(\text{PPh}_3)(\text{CH}=\text{CH}(\text{CH}_2)_{n-2})]^+\text{BF}_4^-$ ; Facile Vinylic Deprotonation of a Coordinated Alkene

James J. Kowalczyk, Atta M. Arif, and J. A. Gladysz\*

Department of Chemistry, University of Utah,  
Salt Lake City, Utah 84112, U.S.A.

Received September 25, 1990

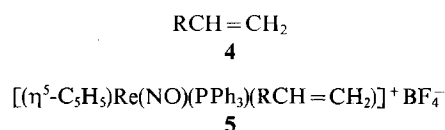
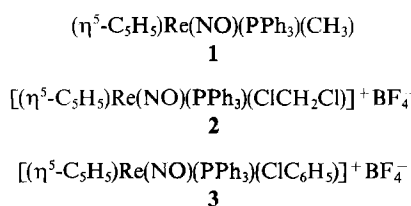
**Key Words:** Cycloalkene ligands / Cyclopentylidene ligands / Deprotonation reactions / Rhenium complexes

Reactions of  $[(\eta^5\text{-C}_5\text{H}_5)\text{Re}(\text{NO})(\text{PPh}_3)(\text{C}(\text{ClC}_6\text{H}_5))]^+\text{BF}_4^-$  and  $\text{CH}=\text{CH}(\text{CH}_2)_{n-2}$  ( $n = 5, \mathbf{a}; 6, \mathbf{b}; 7, \mathbf{c}; 8, \mathbf{d}$ ) give cycloalkene complexes  $[(\eta^5\text{-C}_5\text{H}_5)\text{Re}(\text{NO})(\text{PPh}_3)(\text{CH}=\text{CH}(\text{CH}_2)_{n-2})]^+\text{BF}_4^-$  ( $\mathbf{6a-d}$ , 94 to 79%). A crystal structure of the methylcyclopentadienyl analog of  $\mathbf{6a}$  shows the  $\text{Re}-\text{C}\cdots\text{C}$  plane and  $\text{Re}-\text{PPh}_3$  bond to be coplanar, with the vinyl protons *syn* to the cyclopentadienyl ligand. Reaction of  $\mathbf{6a}$  and  $t\text{BuO}^-\text{K}^+$  leads to the vinyl complex  $(\eta^5\text{-C}_5\text{H}_5)\text{Re}(\text{NO})(\text{PPh}_3)(\text{C}=\text{CH}(\text{CH}_2)_3)$  ( $\mathbf{9a}$ , 90%) instead of expected allyl complex  $(\eta^5\text{-C}_5\text{H}_5)\text{Re}(\text{NO})(\text{PPh}_3)(\text{CH}=\text{CH}(\text{CH}_2)_2)$  ( $\mathbf{10a}$ ). Analogous reactions of  $\mathbf{6b-d}$  give var-

ying mixtures of  $\mathbf{9b-d/10b-d}$ .  $\text{HBF}_4 \cdot \text{OEt}_2$  and  $\mathbf{9a}$  react to form the cyclopentylidene complex  $[(\eta^5\text{-C}_5\text{H}_5)\text{Re}(\text{NO})(\text{PPh}_3)(\text{C}(\text{CH}_2)_4)]^+\text{BF}_4^-$  ( $\mathbf{11}^+ \text{BF}_4^-$ , 96%), the stability of which precludes any intermediacy in the deprotonation of  $\mathbf{6a}$ . A crystal structure of  $\mathbf{11}^+ \text{PF}_6^-$  shows the  $\text{Re}=\text{C}-\text{C}$  planes to be perpendicular to the  $\text{Re}-\text{P}$  bond. Spectroscopic features of compounds  $\mathbf{6}$  are analyzed in detail, and NMR data show a high barrier to cyclopentylidene ligand rotation in  $\mathbf{11}^+ \text{BF}_4^-$  ( $\Delta G^\ddagger$  (110°C)  $\geq 19$  kcal/mol).

Increasing numbers of chiral-at-metal alkene complexes are becoming available in optically active form<sup>1)</sup>. Such compounds offer a variety of potential applications in asymmetric synthesis. Accordingly, we have sought to systematically extend our studies of chiral rhenium complexes  $[(\eta^5\text{-C}_5\text{H}_5)\text{Re}(\text{NO})(\text{PPh}_3)(\text{L})]^+\text{X}^-$  to different classes of alkene ligands.

We recently reported that the reaction of chiral methyl complex  $(\eta^5\text{-C}_5\text{H}_5)\text{Re}(\text{NO})(\text{PPh}_3)(\text{CH}_3)$  ( $\mathbf{1}$ ) and  $\text{HBF}_4 \cdot \text{OEt}_2$  in dichloromethane or chlorobenzene affords the labile chlorocarbon complexes  $[(\eta^5\text{-C}_5\text{H}_5)\text{Re}(\text{NO})(\text{PPh}_3)(\text{ClCH}_2\text{Cl})]^+\text{BF}_4^-$  ( $\mathbf{2}$ ) and  $[(\eta^5\text{-C}_5\text{H}_5)\text{Re}(\text{NO})(\text{PPh}_3)(\text{ClC}_6\text{H}_5)]^+\text{BF}_4^-$  ( $\mathbf{3}$ ), respectively<sup>2,3)</sup>. These react with monosubstituted alkenes  $\text{RCH}=\text{CH}_2$  to give substitution products  $[(\eta^5\text{-C}_5\text{H}_5)\text{Re}(\text{NO})(\text{PPh}_3)(\text{RCH}=\text{CH}_2)]^+\text{BF}_4^-$  ( $\mathbf{5}$ ) in high yields<sup>2-4)</sup>. When optically active  $\mathbf{1}$  is utilized, alkene complexes  $\mathbf{5}$  form with overall retention of configuration at rhenium and in high optical yields<sup>4)</sup>. Hence,  $\mathbf{2}$  and  $\mathbf{3}$  can serve as functional equivalents of the chiral, *optically active*, rhenium Lewis acid  $[(\eta^5\text{-C}_5\text{H}_5)\text{Re}(\text{NO})(\text{PPh}_3)]^+$  ( $\mathbf{I}$ ). Importantly, this moiety is also a strong  $\pi$  donor, with the d orbital HOMO shown in Scheme 1.

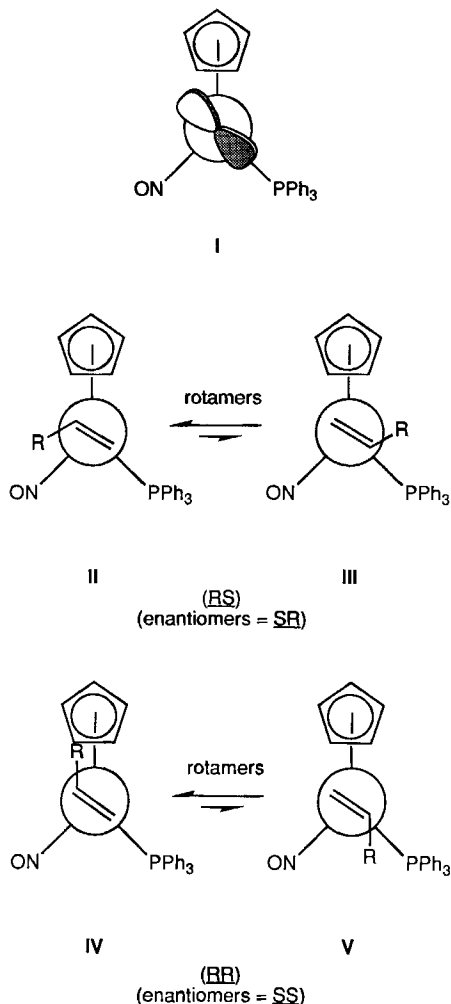


As analyzed in our previous paper<sup>4)</sup>, the  $\text{C}=\text{C}$   $\pi$  faces of simple monosubstituted alkenes are *enantiotopic*. Thus, two configurational diastereomers are possible upon complexation to a chiral metal fragment. Idealized structures of the diastereomers of rhenium monosubstituted alkene complexes  $\mathbf{5}$  are shown in Newman projections  $\mathbf{II-V}$  (Scheme 1). Each diastereomer can exist as two  $\text{Re}-(\text{C}\cdots\text{C})$  rotamers. NMR and structural data show that the rotamers which place the substituted alkene carbon *anti* to the  $\text{PPh}_3$  ligand ( $\mathbf{II, IV}$ ) are more stable. Intuitively, steric interactions between the small nitrosyl ligand and alkene substituent in  $\mathbf{II}$  should be less than those involving the medium-sized cyclopentadienyl ligand in  $\mathbf{IV}$ . Accordingly, equilibration experiments show that the (*RS,SR*) diastereomers are considerably more stable than the (*RR,SS*) diastereomers<sup>5)</sup>. Thus, protocols for the selective binding and activation of one monosubstituted alkene enantioface have been achieved<sup>4,6,7)</sup>.

We sought to extend these studies to cycloalkene complexes of the formula  $[(\eta^5\text{-C}_5\text{H}_5)\text{Re}(\text{NO})(\text{PPh}_3)(\text{CH}=\text{CH}(\text{CH}_2)_{n-2})]^+\text{BF}_4^-$  ( $\mathbf{6}$ ;  $n \geq 5$ ). However, the  $\text{C}=\text{C}$  faces of unsubstituted *cis*-cycloalkenes are *identical*, as opposed to *enantiotopic*. Thus, configurational diastereomers of  $\mathbf{6}$  are not possible. However, two  $\text{Re}-(\text{C}\cdots\text{C})$  rotamers,  $\mathbf{VI}$  and  $\mathbf{VII}$  (Scheme 2), can exist. Based upon the preceding analysis

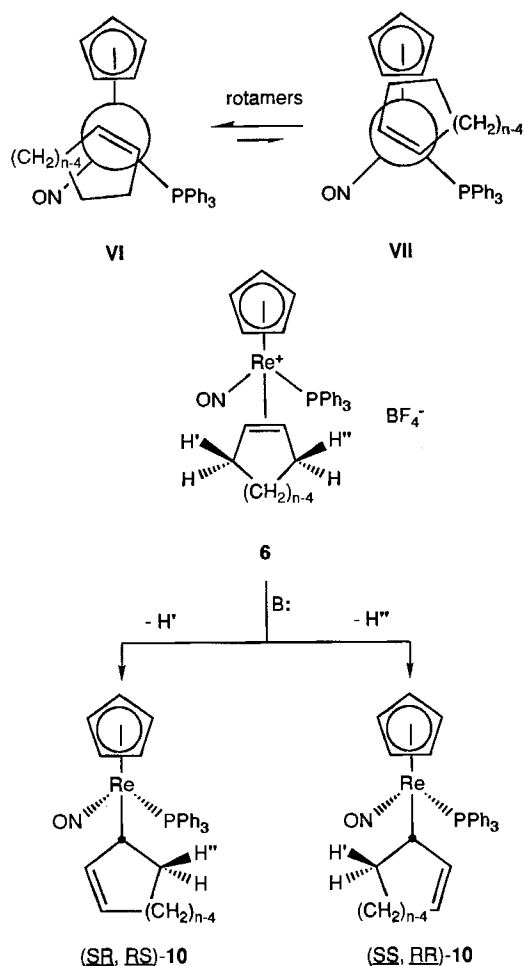
of steric effects in isomers **II**–**V** of monosubstituted alkene complexes **5**, **VI** should be the more stable rotamer of **6**.

Scheme 1. Newman projections showing (**I**) the d orbital HOMO of the  $[(\eta^5\text{-C}_5\text{H}_5)\text{Re}(\text{NO})(\text{PPh}_3)]^+$  fragment and (**II**–**IV**) idealized structures of diastereomeric monosubstituted alkene complexes  $[(\eta^5\text{-C}_5\text{H}_5)\text{Re}(\text{NO})(\text{PPh}_3)(\text{RCH}=\text{CH}_2)]^+\text{X}^-$  (**5**)



Among various possible asymmetric transformations of **6**, our attention was drawn in particular to deprotonation reactions. Cationic alkene complexes commonly undergo allylic deprotonation by mild bases, giving neutral  $\sigma$ -allyl complexes<sup>8</sup>. Proton abstraction occurs from a direction *anti* to the metal. This reaction has been explicitly demonstrated for  $t\text{BuO}^-\text{K}^+$  and rhenium alkene complexes  $[(\eta^5\text{-C}_5\text{H}_5)\text{Re}(\text{NO})(\text{PPh}_3)(\text{H}_2\text{C}=\text{C}(\text{R}')\text{CH}_2\text{R})]^+\text{X}^-$  ( $\text{R}/\text{R}' = \text{H}/\text{H}$ ,  $\text{C}_6\text{H}_5/\text{H}$ ,  $\text{H}/\text{CH}_3$ )<sup>9</sup>. In cycloalkene complexes **6**, there are two inequivalent allylic protons with an *anti* relationship to the rhenium, as sketched in Scheme 2 ( $\text{H}'$ ,  $\text{H}''$ ). Deprotonation generates a new stereocenter in the product ( $\text{C}_\alpha$ ), the configuration of which will be determined by the allylic proton abstracted. Thus, the chiral rhenium Lewis acid **I** provides a potential vehicle for the stereospecific desymmetrization of simple cycloalkenes.

Scheme 2. Newman projections (**VI**, **VII**) of rotamers of cycloalkene complexes  $[(\eta^5\text{-C}_5\text{H}_5)\text{Re}(\text{NO})(\text{PPh}_3)(\text{CH}=\text{CH}(\text{CH}_2)_{n-2})]^+\text{BF}_4^-$  (**6**) and possible allylic deprotonation modes



In this paper we report (a) high-yield syntheses of cycloalkene complexes  $[(\eta^5\text{-C}_5\text{H}_5)\text{Re}(\text{NO})(\text{PPh}_3)(\text{CH}=\text{CH}(\text{CH}_2)_{n-2})]^+\text{BF}_4^-$  (**6**), (b) a detailed analysis of their spectroscopic properties, (c) the crystal structure of a cyclopentene complex, (d) the facile and apparently unprecedented *vinyl*ic deprotonation of a cyclopentene complex, (e) data relevant to the mechanism of vinyl<sup>ic</sup> deprotonation, and (f) a crystal structure of a cyclopentylidene complex.

## Results

### 1. Syntheses of Cycloalkene Complexes

Chlorobenzene complex  $[(\eta^5\text{-C}_5\text{H}_5)\text{Re}(\text{NO})(\text{PPh}_3)(\text{Cl-C}_6\text{H}_5)]^+\text{BF}_4^-$  (**3**; Scheme 3) was generated at  $-45^\circ\text{C}$  as previously described<sup>3</sup>. Then the alkenes (a) cyclopentene, (b) cyclohexene, (c) cycloheptene, and (d) cyclooctene were added (5–10 equiv.). These mixtures were kept for 4–12 hours at room temperature. Workup gave cycloalkene complexes  $[(\eta^5\text{-C}_5\text{H}_5)\text{Re}(\text{NO})(\text{PPh}_3)(\text{CH}=\text{CH}(\text{CH}_2)_{n-2})]^+\text{BF}_4^-$  (**6a–d**;  $n = 5–8$ ) in 94–79% yields as tan or golden powders. When analogous reactions were attempted with dichloromethane complex **2**, isolated yields and product purities were generally lower.

Attempts to obtain samples of **6a–d** that were suitable for X-ray crystallography have been unsuccessful. Preliminary crystallizations of analogous hexafluorophosphate

salts have also been unpromising. Thus, methylcyclopentadienyl derivatives were sought. First, methyl complex ( $\eta^5\text{-C}_5\text{H}_5$ ) $\text{Re}(\text{NO})(\text{PPh}_3)(\text{CH}_3)$  (**1**) was treated with *n*BuLi to gen-

Table 1. Spectroscopic characterization of cycloalkene complexes  $[(\eta^5\text{-C}_5\text{H}_5)\text{Re}(\text{NO})(\text{PPh}_3)(\text{CH}=\text{CH}(\text{CH}_2)_{n-2})]^+\text{BF}_4^-$  (**6**) and other new complexes

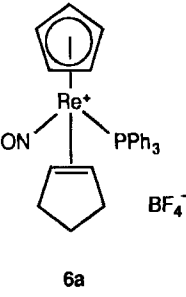
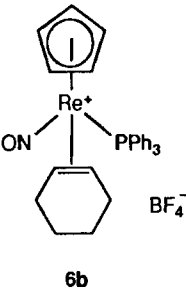
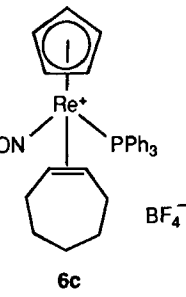
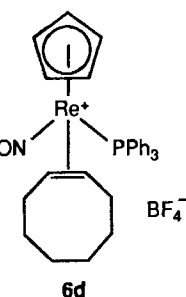
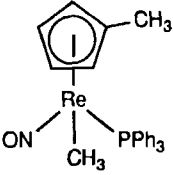
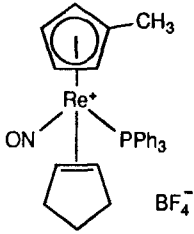
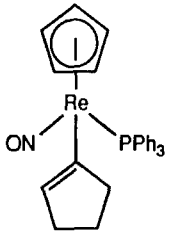
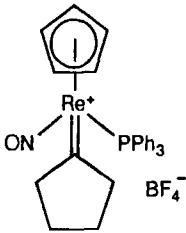
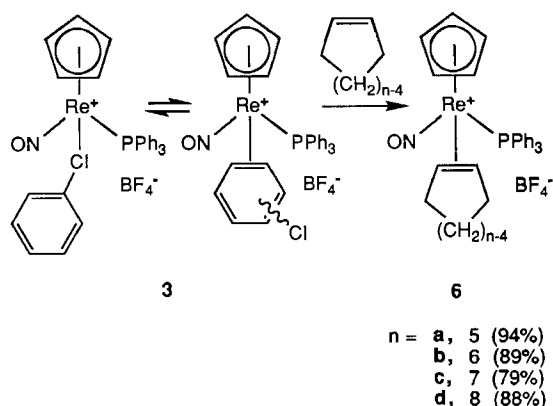
Complex	IR ( $\text{cm}^{-1}$ , KBr)	$^1\text{H}$ NMR <sup>a</sup> ( $\delta$ )	$^{13}\text{C}\{^1\text{H}\}$ NMR <sup>b</sup> ( $\delta$ )	$^{31}\text{P}\{^1\text{H}\}$ NMR <sup>c</sup> ( $\delta$ )
 <p><b>6a</b></p>	$\nu_{\text{NO}}$ 1726 vs	7.57 - 7.64 (m, 9H of 3 $\text{C}_6\text{H}_5$ ), 7.41 - 7.54 (m, 6H of 3 $\text{C}_6\text{H}_5$ ), 5.73 (s, $\text{C}_5\text{H}_5$ ), 4.77 - 4.80 (m, =CH), 4.00 - 4.07 (m, 1H), 3.22 - 3.35 (m, 1H), 2.81 - 2.94 (m, 1H), 2.33 - 2.41 (m, 1H), 1.18 - 1.39 (m, 2H), 0.79 - 0.90 (m, 1H).	PPh <sub>3</sub> at 133.3 (d, $J = 10.1$ , <i>q</i> ), 132.0 (d, $J = 2.5$ , <i>p</i> ), 131.1 (d, $J = 57.0$ , <i>ipso</i> ), 129.4 (d, $J = 11.2$ , <i>m</i> ); 97.2 (s, $\text{C}_5\text{H}_5$ ); C=C at 60.4 (d, $J = 4.8$ , <i>syn</i> to PPh <sub>3</sub> ), 58.0 (s, <i>anti</i> to PPh <sub>3</sub> ); CH <sub>2</sub> at 35.9 (s), 33.4 (s), 20.1 (s).	8.6 (s)
 <p><b>6b</b></p>	$\nu_{\text{NO}}$ 1711 vs	7.54 - 7.59 (m, 9H of 3 $\text{C}_6\text{H}_5$ ), 7.38 - 7.47 (m, 6H of 3 $\text{C}_6\text{H}_5$ ), 5.69 (s, $\text{C}_5\text{H}_5$ ), 4.38 - 4.80 (m, 2H), 3.38 - 3.45 (m, 1H), 2.52 - 2.58 (m, 1H), 1.96 - 2.03 (m, 1H), 1.41 - 1.53 (m, 2H), 1.16 - 1.21 (m, 3H).	PPh <sub>3</sub> at 133.6 (d, $J = 10.0$ , <i>q</i> ), 132.1 (d, $J = 2.3$ , <i>p</i> ), 130.5 (d, $J = 56.9$ , <i>ipso</i> ), 129.5 (d, $J = 10.9$ , <i>m</i> ); 97.3 (s, $\text{C}_5\text{H}_5$ ); C=C at 58.9 (d, $J = 3.7$ , <i>syn</i> to PPh <sub>3</sub> ), 55.5 (s, <i>anti</i> to PPh <sub>3</sub> ); CH <sub>2</sub> at 31.6 (s), 25.4 (s), 22.7 (s), 20.7 (s).	8.5 (s)
 <p><b>6c</b></p>	$\nu_{\text{NO}}$ 1711 vs	7.51 - 7.58 (m, 9H of 3 $\text{C}_6\text{H}_5$ ), 7.34 - 7.47 (m, 6H of 3 $\text{C}_6\text{H}_5$ ), 5.71 (s, $\text{C}_5\text{H}_5$ ), 4.05 - 4.07 (m, =CH), 3.57 - 3.62 (m, 1H), 1.14 - 2.19 (m, 10H).	PPh <sub>3</sub> at 133.4 (d, $J = 9.9$ , <i>q</i> ), 132.0 (d, $J = 2.3$ , <i>p</i> ), 130.7 (d, $J = 57.1$ , <i>ipso</i> ), 129.4 (d, $J = 11.0$ , <i>m</i> ); 97.4 (s, $\text{C}_5\text{H}_5$ ); C=C at 57.1 (br s, <i>syn</i> to PPh <sub>3</sub> ), 54.5 (br s, <i>anti</i> to PPh <sub>3</sub> ); CH <sub>2</sub> at 33.7 (s), 31.8 (s), 31.4 (br s), 29.8 (s), 29.4 (s).	5.9 (s)
 <p><b>6d</b></p>	$\nu_{\text{NO}}$ 1710 vs	7.55 - 7.56 (m, 9H of 3 $\text{C}_6\text{H}_5$ ), 7.31 - 7.36 (m, 6H of 3 $\text{C}_6\text{H}_5$ ), 5.72 (s, $\text{C}_5\text{H}_5$ ), 4.21 - 4.27 (br m, =CH), 2.80 - 2.87 (br m, 1H), 0.87 - 2.20 (m, 12H).	PPh <sub>3</sub> at 133.5 (d, $J = 10.2$ , <i>q</i> ), 131.9 (d, $J = 2.4$ , <i>p</i> ), 130.1 (d, $J = 56.7$ , <i>ipso</i> ), 129.3 (d, $J = 10.6$ , <i>m</i> ); 97.5 (s, $\text{C}_5\text{H}_5$ ); C=C at 57.7 (s, <i>syn</i> to PPh <sub>3</sub> ), 56.1 (br s, <i>anti</i> to PPh <sub>3</sub> ); CH <sub>2</sub> at 33.7 (s), 33.5 (s), 32.5 (v br s), 29.2 (v br s), 26.0 (s), 25.2 (s).	9.0 (s)

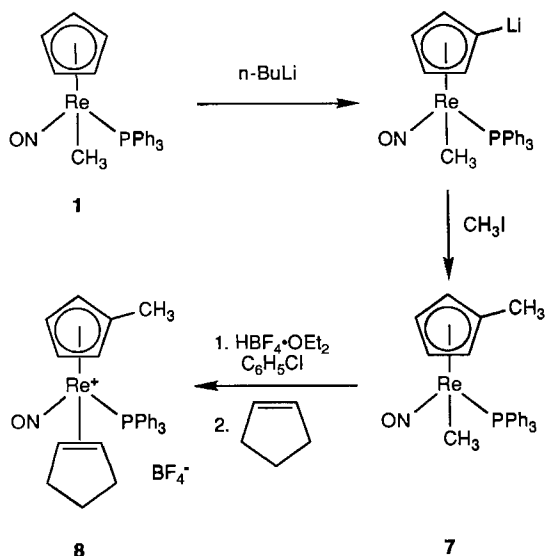
Table 1 (Continued)

Complex	IR (cm <sup>-1</sup> , KBr)	<sup>1</sup> H NMR <sup>a</sup> (δ)	<sup>13</sup> C{ <sup>1</sup> H} NMR <sup>b</sup> (δ)	<sup>31</sup> P{ <sup>1</sup> H} NMR <sup>c</sup> (δ)
 <p>7</p>	ν <sub>NO</sub> 1621 vs	7.38 - 7.46 (m, 3C <sub>6</sub> H <sub>5</sub> ); C <sub>5</sub> H <sub>4</sub> at 5.24 (br s, 1H), 4.90 (br s, 1H), 4.70 (br d, J = 2.2, 1H), 3.79 (br d, J = 1.9, 1 H); 1.87 (s, CCH <sub>3</sub> ), 0.92 (d, J <sub>HP</sub> = 5.8, ReCH <sub>3</sub> ).	PPh <sub>3</sub> at 136.4 (d, J = 50.7, <i>ipso</i> ), 133.5 (d, J = 11.0, <i>o</i> ), 129.7 (s, <i>p</i> ), 128.1 (d, J = 10.1, <i>m</i> ); C <sub>5</sub> H <sub>4</sub> at 109.2 (s), 92.0 (s), 87.3 (s), 86.1 (s), 84.6 (d, J = 3.5); 13.4 (s, CCH <sub>3</sub> ), -30.9 (d, J = 6.7, ReCH <sub>3</sub> ).	25.9 (s)
 <p>8</p>	ν <sub>NO</sub> 1722 vs	7.54 - 7.62 (m, 9H of 3 C <sub>6</sub> H <sub>5</sub> ), 7.40 - 7.48 (m, 6H of 3 C <sub>6</sub> H <sub>5</sub> ); C <sub>5</sub> H <sub>4</sub> at 6.13 (br s, 1H), 5.35 (br s, 1H), 5.11 - 5.14 (2 br s, 2H); 4.64 - 4.67 (m, =CH), 3.90 - 3.97 (m, 1H), 3.24 - 3.36 (m, 1H), 2.82 - 2.95 (m, 1H), 2.30 - 2.38 (m, 1H), 2.25 (s, CH <sub>3</sub> ), 1.18 - 1.40 (m, 2H), 0.82 - 0.93 (m, 1H).	PPh <sub>3</sub> at 133.4 (d, J = 10.0, <i>o</i> ), 132.0 (d, J = 2.9, <i>p</i> ), 130.6 (d, J = 57.1, <i>ipso</i> ), 129.5 (d, J = 10.1, <i>m</i> ); C <sub>5</sub> H <sub>4</sub> at 114.9 (s), 98.5 (s), 98.4 (s), 97.2 (s), 91.3 (s); C=C at 61.1 (d, J = 5.2, <i>syn</i> to PPh <sub>3</sub> ), 58.6 (s, <i>anti</i> to PPh <sub>3</sub> ); CH <sub>2</sub> at 35.7 (s), 33.4 (s), 20.0 (s); 12.7 (s, CH <sub>3</sub> ).	9.2 (s)
 <p>9a</p>	ν <sub>NO</sub> 1632 vs	7.33 - 7.43 (m, 3C <sub>6</sub> H <sub>5</sub> ), 5.05 (s, C <sub>5</sub> H <sub>5</sub> ), 4.77 - 4.78 (m, =CH), 2.35 - 2.05 (m, 4H), 1.40 - 1.50 (m, 1H), 1.22 - 1.33 (m, 1H). <sup>d</sup>	PPh <sub>3</sub> at 136.5 (d, J = 52.5, <i>ipso</i> ), 133.8 (d, J = 10.7, <i>o</i> ), 130.0 (s, <i>p</i> ), 128.1 (d, J = 10.6, <i>m</i> ); 90.5 (s, C <sub>5</sub> H <sub>5</sub> ); C=C at 138.5 (d, J = 9.8, ReC=C), 133.0 (s, ReC=C); CH <sub>2</sub> at 50.3 (s), 35.3 (s), 25.7 (s). <sup>d</sup>	21.0 (s) <sup>d</sup>
 <p>11<sup>+</sup> BF<sub>4</sub><sup>-</sup></p>	ν <sub>NO</sub> 1716 vs	7.57 - 7.59 (m, 9H of 3 C <sub>6</sub> H <sub>5</sub> ), 7.26 - 7.35 (m, 6H of 3 C <sub>6</sub> H <sub>5</sub> ), 5.95 (s, C <sub>5</sub> H <sub>5</sub> ), 2.99 - 3.24 (m, 2H), 2.75 - 2.86 (m, 1H), 2.45 - 2.56 (m, 1H), 1.38 - 1.77 (m, 3H), 1.08 - 1.26 (m, 1H).	PPh <sub>3</sub> at 132.8 (d, J = 10.9, <i>o</i> ), 132.4 (s, <i>p</i> ), 129.6 (d, J = 60.1, <i>ipso</i> ), 129.6 (d, J = 11.6, <i>m</i> ); 98.7 (s, C <sub>5</sub> H <sub>5</sub> ); 332.2 (d, J = 6.5, Re=C), CH <sub>2</sub> at 61.7 (s), 60.9 (s), 27.5 (s), 26.8 (s).	14.8 (s)

<sup>a</sup> At 300 MHz in CDCl<sub>3</sub> at ambient probe temperature and referenced to internal Si(CH<sub>3</sub>)<sub>4</sub> (δ = 0.00) unless noted; couplings [Hz] are to hydrogen unless noted. — <sup>b</sup> At 75.4 MHz in CDCl<sub>3</sub> at ambient probe temperature and referenced to CDCl<sub>3</sub> (δ = 77.0) unless noted; couplings [Hz] are to phosphorus. — <sup>c</sup> At 121 MHz in CDCl<sub>3</sub> at ambient probe temperature and referenced to external 85% H<sub>3</sub>PO<sub>4</sub> (δ = 0.00). — <sup>d</sup> Spectrum recorded in CD<sub>2</sub>Cl<sub>2</sub>.

Scheme 3. Synthesis of cycloalkene complexes  $[(\eta^5\text{-C}_5\text{H}_5)\text{Re}(\text{NO})\text{-(PPh}_3)_2(\text{CH}=\text{CH}(\text{CH}_2)_{n-2})]^+\text{BF}_4^-$  (**6**)

erate lithiocyclopentadienyl complex  $(\eta^5\text{-C}_5\text{H}_4\text{Li})\text{Re}(\text{NO})\text{-(PPh}_3)_2(\text{CH}_3)$  as previously described (Scheme 4)<sup>10</sup>. Then methyl iodide was added. Workup gave the new methylcyclopentadienyl complex **7** in 82% yield. Complex **7** was then dissolved in chlorobenzene and sequentially treated with  $\text{HBF}_4 \cdot \text{OEt}_2$  and cyclopentene at  $-45^\circ\text{C}$ . Workup gave cyclopentene complex **8** in 88% yield. X-ray quality crystals of **8** were readily obtained.

Scheme 4. Synthesis of methylcyclopentadienyl complexes **7**, **8**

## 2. Spectroscopic Properties of Cycloalkene Complexes

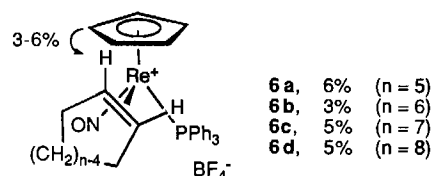
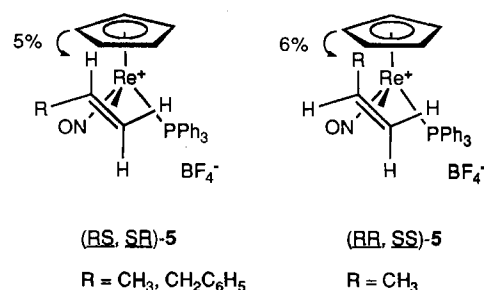
The new complexes **6a–d**, **7**, and **8** were characterized by microanalysis, and IR and NMR ( $^1\text{H}$ ,  $^{13}\text{C}\{^1\text{H}\}$ ,  $^{31}\text{P}\{^1\text{H}\}$ ) spectroscopy (Table 1). Cycloalkene complexes **6a–d** and **8** exhibited IR  $\nu_{\text{NO}}$  and  $\text{PPh}_3$  ligand  $^{31}\text{P}$ -NMR chemical shifts that were similar to those of monosubstituted alkene complexes **5**<sup>4</sup>. Complexes **7** and **8** gave  $^1\text{H}$ - and  $^{13}\text{C}$ -NMR resonance patterns that were characteristic of methylcyclopentadienyl ligands<sup>11</sup>.

The  $\text{C}=\text{C}$   $^{13}\text{C}$ -NMR resonances in **6a–d** and **8** ( $\delta = 55\text{--}61$ ) were shifted upfield from those of the corresponding

free cycloalkenes and into a range commonly observed for coordinated alkenes (Table 1)<sup>12</sup>. One  $\text{C}=\text{C}$  resonance was consistently 2–4 ppm downfield of the other, and usually exhibited a larger  $^2J_{\text{CP}}$ . In monosubstituted alkene complexes **5**, the  $\text{C}=\text{C}$  carbons *syn* to the  $\text{PPh}_3$  ligand have been shown to exhibit a larger  $^2J_{\text{CP}}$  (4–6 Hz) than those that are *anti* ( $<2$  Hz)<sup>4</sup>. An analogous trend has been found for the  $\text{C}\equiv\text{C}$  carbons of corresponding alkyne complexes<sup>13</sup>. Hence, the downfield  $\text{C}=\text{C}$   $^{13}\text{C}$ -NMR resonances of **6a–d** and **8** were assigned to the carbons *syn* to the  $\text{PPh}_3$  ligand.

A  $^{13}\text{C}$ -NMR spectrum of **6a** was recorded without proton decoupling. The  $\text{C}=\text{C}$  carbons exhibited  $^1J_{\text{CH}}$  of 166–167 Hz (d). The remaining cyclopentene ligand carbons gave  $^1J_{\text{CH}}$  of 130–133 Hz (t). The corresponding  $^1J_{\text{CH}}$  for cyclopentene ( $=\text{CH}$ ), ethylene, and ethane are 162, 156, and 125 Hz, respectively<sup>14</sup>. Although  $^1J_{\text{CH}}$  values are diagnostic of carbon hybridization<sup>14</sup>, it should be emphasized that they are not considered reliable indicators of metallacyclopentane character in metal alkene complexes<sup>15</sup>.

Difference  $^1\text{H}$ -NOE experiments<sup>16</sup> have been previously conducted with monosubstituted alkene complexes **5**<sup>4</sup>. As illustrated in Scheme 5, cyclopentadienyl ligand irradiation enhances the resonances of groups that are *syn* to the cyclopentadienyl ligand on the  $\text{C}=\text{C}$  carbon *anti* to the  $\text{PPh}_3$  ligand. Complexes **6a–d** and **8** generally gave well-separated vinyl proton resonances (Table 1), and analogous NOE experiments were conducted in  $\text{CDCl}_3$  as summarized in Scheme 5. Only the downfield vinyl proton resonances were enhanced. Accordingly, these were assigned to the vinyl protons on the  $\text{C}=\text{C}$  carbons *anti* to the  $\text{PPh}_3$  ligand, as shown in Scheme 5. Some enhancement of the  $\text{PPh}_3$  ligand *ortho* protons was also observed.

Scheme 5. Summary of data from  $^1\text{H}$  difference NOE experiments on monosubstituted alkene complexes **5** and cycloalkene complexes **6** (from cyclopentadienyl ligand irradiation)

As a check on the preceding NMR assignments, the downfield vinyl protons of **6a, d** ( $\delta = 4.78, 4.23$ ) were selectively irradiated while a  $^{13}\text{C}$ -NMR spectrum was recorded. In each

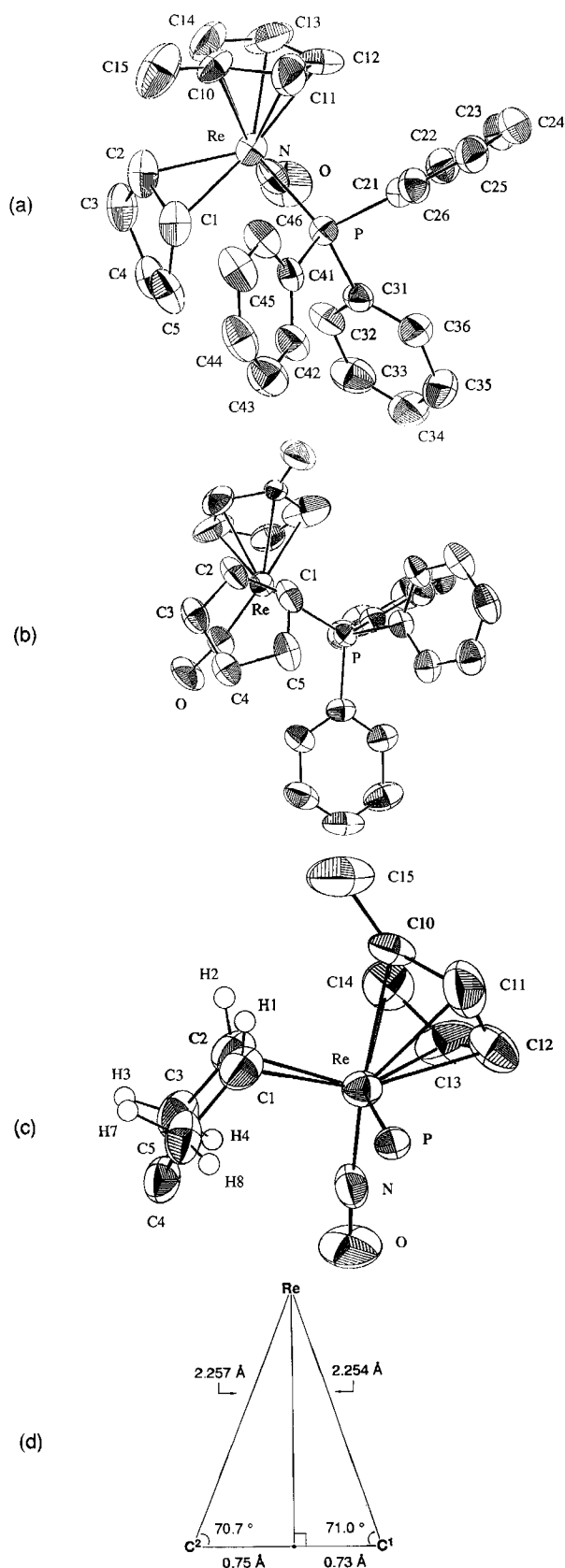


Figure 1. Structure of the cation of cyclopentene complex  $[(\eta^5\text{-C}_5\text{H}_4\text{CH}_3)\text{Re}(\text{NO})(\text{PPh}_3)(\text{CH}=\text{CH}(\text{CH}_2)_3)]^+\text{BF}_4^-$  (**8**). (a) Numbering diagram. (b) Newman-type projection. (c) Side view of cyclopentene ligand. (d) View of  $\text{Re}-\text{C}\cdots\text{C}$  plane

case, the upfield  $\text{C}=\text{C}$  resonances ( $\delta = 58.0, 56.1$ ) were singlets, while the downfield resonances showed large couplings ( $^1J_{\text{CH}}$ ). This confirms that the downfield vinyl protons are bound to the upfield  $\text{C}=\text{C}$  carbons.

### 3. Crystal Structure of Cyclopentene Complex **8**

The preceding NOE data indicate that rotamer **VI** of cycloalkene complexes **6a–d** is considerably more stable than rotamer **VII** (Scheme 2). A crystallographic confirmation was also sought. Thus, X-ray data were collected on cyclopentene complex **8** as summarized in Table 2. Refinement, described in the experimental section, gave the structures shown in Figure 1. All cyclopentene ligand hydrogens were located. Atomic coordinates, and key bond lengths, bond angles, and torsion angles, are given in Tables 3, 4.

Figure 1b shows that **8** adopts a  $\text{Re}-(\text{C}\cdots\text{C})$  conformation very close to that of idealized rotamer **VI**. In **VI**, the  $\text{Re}-\text{C}\cdots\text{C}$  plane defines angles of 0 and  $90^\circ$ , respectively, with the  $\text{Re}-\text{P}$  and  $\text{Re}-\text{N}$  bonds. In **8**, corresponding angles of  $8.8$  and  $73.6^\circ$  ( $\equiv 106.4^\circ$ ) are found. The  $\text{Re}-\text{C}\cdots\text{C}$

Table 2. Crystallographic data for cyclopentene complex  $[(\eta^5\text{-C}_5\text{H}_4\text{CH}_3)\text{Re}(\text{NO})(\text{PPh}_3)(\text{CH}=\text{CH}(\text{CH}_2)_3)]^+\text{BF}_4^-$  (**8**) and cyclopentylidene complex  $[(\eta^5\text{-C}_5\text{H}_5)\text{Re}(\text{NO})(\text{PPh}_3)(\text{C}(\text{CH}_2)_4)]^+\text{PF}_6^-$  (**11** +  $\text{PF}_6^-$ )

	<b>8</b>	<b>11</b> + $\text{PF}_6^-$
molecular formula	$\text{C}_{29}\text{H}_{30}\text{BF}_4\text{NOPRe}$	$\text{C}_{28}\text{H}_{28}\text{F}_6\text{NOP}_2\text{Re}$
formula weight	712.547	756.680
crystal system	orthorhombic	monoclinic
space group	$\text{Pna}2_1$ (#33)	$\text{P}2_1/\text{c}$ (#14)
cell dimensions		
$a$ , Å	18.815(2)	9.087(1)
$b$ , Å	10.872(1)	15.666(3)
$c$ , Å	13.534(1)	19.767(2)
$\beta$ , deg		96.24(1)
$V$ , Å <sup>3</sup>	2768.40	2797.34
$Z$	4	4
temp of collection	16(1)°C	16(1)°C
$d_{\text{calcd}}$ , g/cm <sup>3</sup>	1.709	1.797
$d_{\text{obsd}}$ , g/cm <sup>3</sup> (23 °C)	1.68	1.77
crystal dimensions, mm	0.35 x 0.32 x 0.20	0.33 x 0.26 x 0.23
radiation, Å	$\lambda(\text{Mo K}\alpha)$ 0.71073	$\lambda(\text{Cu K}\alpha)$ 1.54056
data collection method	$\theta/2\theta$	$\theta/2\theta$
scan speed, deg/min	3.0	variable
range/indices ( $h,k,l$ )	0,22 0,12 -16,0	0,10 0,18 -23,23
scan range	$\text{K}\alpha_1$ -1.3 to $\text{K}\alpha_2$ +1.6	$0.80 + 0.14 \tan\theta$
total bkdg. time/scan time	0	0
no. of reflections between std.	98	1 x-ray hour
total unique data	2784	4634
observed data $I > 3\sigma(I)$	2170	4009
abs. coefficient ( $\mu$ ), cm <sup>-1</sup>	45.54	98.55
minimum transmission factor	0.8899	0.7177
maximum transmission factor	0.9999	0.9991
no. of variables	342	353
goodness of fit	2.4210	2.3415
$R = \Sigma  F_o  -  F_c   / \Sigma F_o $	0.0266	0.0319
$R_w = [\Sigma w( F_o  -  F_c )^2 / \Sigma w F_o ^2]^{1/2}$	0.0319	0.0339
$\Delta/\sigma$ (max)	0.011	0.008
$\Delta\rho$ (max), eÅ <sup>-3</sup>	1.009	1.309

Table 3. Atomic coordinates and equivalent isotropic thermal parameters for non-hydrogen atoms in **8** and **11<sup>+</sup>PF<sub>6</sub><sup>-</sup>**. Atoms refined anisotropically are given in the form of the isotropic equivalent displacement parameter defined as:  $(4/3)[a^2B_{11} + b^2B_{22} + c^2B_{33} + ab(\cos\gamma)B_{12} + ac(\cos\beta)B_{13} + bc(\cos\alpha)B_{23}]$

Atom	x	y	z	B(Å <sup>2</sup> )
<b>8:</b>				
Re	0.90296(2)	0.81330(3)	1.000	3.198(6)
P	0.9689(1)	0.7197(2)	1.1356(2)	2.68(5)
F1	0.2848(4)	0.7174(9)	0.6732(8)	7.6(2)
F2	0.1782(5)	0.671(1)	0.7205(7)	10.2(3)
F3	0.2082(6)	0.639(1)	0.5689(8)	12.7(4)
F4	0.1980(7)	0.827(1)	0.622(1)	11.7(4)
O	0.9665(5)	1.0582(6)	1.0184(9)	6.4(3)
N	0.9472(4)	0.9555(7)	1.0128(7)	3.7(2)
C1	0.9806(7)	0.699(1)	0.9123(9)	4.4(3)
C2	0.9414(8)	0.781(1)	0.8442(8)	4.5(3)
C3	0.9930(8)	0.876(1)	0.8012(9)	4.9(3)
C4	1.0636(7)	0.862(1)	0.8566(9)	4.3(3)
C5	1.0596(7)	0.732(1)	0.9049(9)	4.7(3)
C10	0.8042(5)	0.696(1)	0.9519(8)	3.5(2)
C11	0.8030(8)	0.701(2)	1.065(1)	7.6(5)
C12	0.8000(6)	0.826(1)	1.090(1)	5.4(3)
C13	0.7921(6)	0.900(1)	0.997(2)	6.7(3)
C14	0.7945(7)	0.824(1)	0.9172(9)	5.5(3)
C15	0.8025(9)	0.581(1)	0.886(1)	7.2(4)
C21	0.9146(5)	0.710(1)	1.2460(7)	3.0(2)
C22	0.8932(6)	0.819(1)	1.2900(9)	4.2(2)
C23	0.8480(7)	0.817(1)	1.3719(9)	5.0(3)
C24	0.8248(7)	0.704(1)	1.4110(9)	5.3(3)
C25	0.8481(6)	0.595(1)	1.3685(9)	4.6(3)
C26	0.8911(6)	0.598(1)	1.2844(8)	3.8(2)
C31	1.0469(5)	0.801(1)	1.1842(8)	3.2(2)
C32	1.0850(5)	0.884(1)	1.1266(9)	3.8(2)
C33	1.1478(6)	0.935(1)	1.165(1)	5.2(3)
C34	1.1718(7)	0.905(1)	1.259(1)	5.6(3)
C35	1.1355(7)	0.825(1)	1.316(1)	5.7(3)
C36	1.0702(6)	0.773(1)	1.2793(9)	4.2(3)
C41	1.0019(5)	0.5635(9)	1.1165(7)	3.0(2)
C42	1.0713(6)	0.533(1)	1.1334(9)	4.1(2)
C43	1.0956(7)	0.413(1)	1.119(1)	5.2(3)
C44	1.0478(7)	0.325(1)	1.087(1)	5.0(3)
C45	0.9774(7)	0.357(1)	1.069(1)	5.1(3)
C46	0.9560(6)	0.474(1)	1.0832(9)	4.0(3)
B	0.2147(8)	0.719(2)	0.648(1)	5.0(3)

**11<sup>+</sup>PF<sub>6</sub><sup>-</sup>:**

Re	0.07915(3)	0.19229(2)	0.17104(1)	2.801(4)
P1	-0.1557(2)	0.16018(9)	0.20961(7)	2.68(3)
P2	0.4019(2)	0.1815(1)	0.45972(9)	5.02(4)
F1	0.402(1)	0.2497(5)	0.0164(4)	14.3(2)
F2	0.3136(7)	0.3783(4)	0.0041(3)	10.3(2)
F3	0.3855(7)	0.1152(4)	0.3982(3)	11.5(2)
F4	0.2516(6)	0.2240(4)	0.4254(3)	10.7(2)
F5	0.5521(7)	0.1458(6)	0.4931(4)	13.0(2)
F6	0.4882(7)	0.2411(5)	0.4145(4)	12.9(2)
O	0.1665(7)	0.0118(3)	0.1747(3)	8.0(2)
N	0.1261(6)	0.0840(3)	0.1710(3)	4.3(1)
C1	-0.0005(6)	0.1929(4)	0.0756(3)	3.5(1)
C2	-0.0408(8)	0.2704(4)	0.0292(3)	4.5(1)
C3	-0.120(1)	0.2361(6)	-0.0346(4)	7.6(2)
C4	-0.078(1)	0.1476(7)	-0.0408(4)	9.1(3)
C5	-0.0256(9)	0.1171(5)	0.0296(3)	5.2(2)
C10	0.2067(8)	0.3161(5)	0.1566(4)	5.8(2)
C11	0.2988(7)	0.2620(5)	0.1975(4)	5.9(2)
C12	0.2403(8)	0.2512(5)	0.2591(4)	5.5(2)
C13	0.1096(8)	0.2955(5)	0.2561(3)	5.6(2)
C14	0.0883(8)	0.3370(4)	0.1910(4)	5.0(2)
C21	-0.1419(6)	0.1085(3)	0.2926(3)	2.9(1)
C22	-0.2711(7)	0.0821(4)	0.3191(3)	3.9(1)
C23	-0.2612(7)	0.0412(4)	0.3812(3)	4.5(1)
C24	-0.1274(8)	0.0253(4)	0.4167(3)	4.8(2)
C25	0.0004(8)	0.0496(5)	0.3912(3)	4.9(2)
C26	-0.0065(7)	0.0910(4)	0.3287(3)	3.7(1)
C31	-0.2717(6)	0.0854(4)	0.1583(3)	3.2(1)
C32	-0.2249(8)	0.0015(4)	0.1552(4)	5.0(2)
C33	-0.311(1)	-0.0581(4)	0.1179(4)	5.9(2)
C34	-0.4445(9)	-0.0368(5)	0.0849(3)	5.9(2)
C35	-0.4926(8)	0.0456(6)	0.0872(4)	5.8(2)
C36	-0.4067(7)	0.1070(5)	0.1232(3)	4.4(1)
C41	-0.2644(6)	0.2566(4)	0.2160(3)	3.3(1)
C42	-0.3036(7)	0.2852(4)	0.2785(3)	4.1(1)
C43	-0.3763(9)	0.3611(5)	0.2819(4)	5.9(2)
C44	-0.4106(8)	0.4090(5)	0.2247(5)	6.7(2)
C45	-0.3762(8)	0.3824(5)	0.1618(4)	5.7(2)
C46	-0.3023(7)	0.3058(4)	0.1584(4)	4.7(1)

moiety exhibits nearly equal Re—C bond lengths [2.254(9) and 2.257(8) Å] and Re—C...C bond angles [71.0(5), 70.7(5)°], indicating negligible “slippage” of the alkene ligand (Figure 1d).

Table 4. Selected bond lengths [Å], bond angles [°], and torsion angles [°] in **8** and **11<sup>+</sup>PF<sub>6</sub><sup>-</sup>**

<b>8</b>									
Re	P	2.439(2)	N	O	1.177(7)				
Re	N	1.764(6)	C1	C2	1.48(1)				
Re	C1	2.254(9)	C1	C5	1.53(1)				
Re	C2	2.257(8)	C2	C3	1.53(1)				
Re	C10	2.34(1)	C3	C4	1.53(2)				
Re	C11	2.41(2)	C4	C5	1.56(1)				
Re	C12	2.29(1)	C10	C11	1.53(1)				
Re	C13	2.291(7)	C10	C14	1.48(2)				
Re	C14	2.33(1)	C10	C15	1.54(2)				
P	C21	1.813(7)	C11	C12	1.40(2)				
P	C31	1.835(7)	C12	C13	1.50(2)				
P	C41	1.826(7)	C13	C14	1.36(2)				
Re	C1	C2	71.0(5)	C2	C3	C4	107.1(8)		
Re	C1	C5	122.5(6)	C3	C4	C5	104.8(8)		
Re	C1	H1	109.8(6)	C10	C11	C12	106(2)		
Re	C2	C1	70.7(5)	C11	C12	C13	109(2)		
Re	C2	C3	116.9(5)	C12	C13	C14	109.6(8)		
Re	C2	H2	113.7(7)	C13	C14	C10	109(1)		
Re	C1	C1	80.6(3)	C14	C10	C11	106(2)		
P	Re	C2	118.4(3)	C11	C10	C15	128(1)		
N	Re	C1	103.2(3)	C14	C10	C15	125(1)		
N	Re	C2	94.4(4)	Re	P	C21	111.0(2)		
C1	Re	C2	38.3(3)	Re	P	C31	118.3(3)		
P	Re	N	93.0(3)	Re	P	C41	117.0(2)		
Re	N	O	169.6(6)	C21	P	C31	100.6(3)		
C1	C2	C3	109.1(8)	C21	P	C41	104.6(3)		
C1	C2	H2	95.8(8)	C31	P	C41	103.3(3)		
C1	C5	C4	106.4(8)	H3	C3	H4	138.5(8)		
C2	C1	C5	107.7(7)	H5	C4	H6	113.4(9)		
C2	C1	H1	119.0(9)	H7	C5	H8	98.3(6)		
Re	C1	C2	C3	113(1)	P	Re	C1	C2	-171(1)
C5	C1	C2	Re	-119(1)	P	Re	C2	C1	10(1)
Re	C1	C2	H2	-113(1)	N	Re	C1	C2	-80(1)
H1	C1	C2	Re	103(1)	N	Re	C2	C1	106(1)
Re	C1	C5	H7	-176(1)	C2	C3	C4	C5	17(1)
Re	C1	C5	H8	81(1)	C5	C1	C2	C3	-6(1)
Re	C2	C3	H3	157(1)	H1	C1	C2	H2	-10(2)
Re	C2	C3	H4	-52(1)					
<b>11<sup>+</sup>PF<sub>6</sub><sup>-</sup></b>									
Re	C1	1.945(4)	N	O	1.189(5)				
Re	C10	2.294(4)	C1	C2	1.542(6)				
Re	C11	2.286(4)	C1	C5	1.499(6)				
Re	C12	2.340(5)	C2	C3	1.484(7)				
Re	C13	2.326(4)	C3	C4	1.447(9)				
Re	C14	2.301(4)	C4	C5	1.498(7)				
Re	N	1.749(4)	C10	C11	1.388(7)				
Re	P1	2.3960(9)	C10	C14	1.374(7)				
P1	C21	1.823(4)	C11	C12	1.391(7)				
P1	C31	1.811(4)	C12	C13	1.371(7)				
P1	C41	1.818(4)	C13	C14	1.435(7)				
Re	C1	C2	128.3(3)	C10	C11	C12	108.7(5)		
Re	C1	C5	127.0(3)	C11	C12	C13	108.1(5)		
Re	N	O	175.1(4)	C12	C13	C14	107.5(4)		
P1	Re	N	91.3(1)	C13	C14	C10	107.4(4)		
P1	Re	C1	93.4(1)	C14	C10	C11	108.1(4)		
N	Re	C1	94.0(2)	Re	P1	C21	113.8(1)		
C1	C2	C3	106.4(4)	Re	P1	C31	116.2(1)		
C1	C5	C4	108.8(4)	Re	P1	C41	110.9(1)		
C2	C1	C5	104.6(3)	C21	P1	C31	101.3(2)		
C2	C3	C4	108.1(5)	C21	P1	C41	106.9(2)		
C3	C4	C5	106.7(5)	C31	P1	C41	106.8(2)		
Re	C1	C2	C3	-171(1)	C1	C2	C3	C4	-23(1)
Re	C1	C5	C4	-176(1)	C2	C1	C5	C4	0(1)
N	Re	C1	C2	-167(1)	C2	C3	C4	C5	23(1)
N	Re	C1	C5	8(1)	C3	C4	C5	C1	-14(1)
P1	Re	C1	C2	101(1)	C5	C1	C2	C3	14(1)
P1	Re	C1	C5	-84(1)					

Other geometric features of **8** were calculated. First, the angle of the  $\text{Re}-\text{C}\cdots\text{C}$  plane with the plane defined by the cyclopentadienyl centroid, rhenium, and  $\text{C}\cdots\text{C}$  centroid was  $62.9^\circ$ . This provides an alternative measure of the alkene ligand tilt in Newman projections such as **VI**. Second, the homoallylic carbon C4 was displaced  $0.33 \text{ \AA}$  from the least-squares plane of the remaining cyclopentene ligand carbons (C1, C2, C3, C5), giving an envelope-like conformation. The deviations of C1, C2, C3, and C5 from this plane were less than  $0.04 \text{ \AA}$ . Locations of the hydrogen atoms attached to these carbons are illustrated in Figure 1c.

The alkene carbon substituents in **8** were all markedly bent out of the  $\pi$  nodal plane of the free alkene. This feature was quantified in several ways. First, a plane was defined that contained C2 and C1 but was perpendicular to the  $\text{Re}-\text{C}\cdots\text{C}$  plane. The angles of the C2–C3, C1–C5, C2–H2, and C1–H1 bonds with this plane were  $22, 28, 22,$  and  $11^\circ$ , respectively. This plane also made a  $26^\circ$  angle with the C5–C1–C2–C3 least-squares plane. All of these angles would be  $0^\circ$  in an idealized  $\text{sp}^2$ -hybridized alkene. Finally, the more informative but derivationally more complex  $\alpha$ ,  $\beta$ , and  $\beta'$  angles utilized by Ibers were also calculated ( $79, 51, 31^\circ$ )<sup>17</sup>.

#### 4. Reaction of Cyclopentene Complex **6a** and $t\text{BuO}^- \text{K}^+$

Comensurate with the objectives outlined in Scheme 2, we sought to elaborate the cycloalkene ligands in **6a–d** into allyl ligands. Thus, **6a** was suspended in THF and treated with  $t\text{BuO}^- \text{K}^+$  (Scheme 6). Workup gave a neutral product (90%), which was characterized as described for the other new complexes above. Surprisingly, the data more closely matched that expected for a *vinyl*<sup>18</sup> complex (Table 1). Thus, a  $^{13}\text{C}$ -NMR spectrum was recorded with off-resonance proton decoupling. Only one  $\text{C}=\text{C}$  resonance gave a doublet, diagnostic of a directly-bound hydrogen. Both  $\text{C}=\text{C}$  carbons would bear a hydrogen in the target allyl complex

(Scheme 2). All three aliphatic carbons gave triplets, indicative of two directly-bound hydrogens. Thus, the product was assigned as cyclopentenyl complex  $(\eta^5\text{-C}_5\text{H}_5)\text{Re}(\text{NO})(\text{PPh}_3)(\text{C}=\text{CH}(\text{CH}_2)_3)$  (**9a**). Vinyl complexes of the formula  $(\eta^5\text{-C}_5\text{H}_5)\text{Re}(\text{NO})(\text{PPh}_3)(\text{CH}=\text{CHR})$  have been previously synthesized and their physical and chemical properties studied in detail<sup>7b,18</sup>.

No sign of the alternative deprotonation product, allyl complex  $(\eta^5\text{-C}_5\text{H}_5)\text{Re}(\text{NO})(\text{PPh}_3)(\text{CHCH}=\text{CHCH}_2\text{CH}_2)$  (**10a**), was noted when the reaction of **6a** and  $t\text{BuO}^- \text{K}^+$  was monitored by  $^{31}\text{P}$  NMR. Further, other observations suggested that a spontaneous isomerization of **10a** to **9a** was unlikely. First, several pairs of isomeric vinyl and allyl complexes have been isolated in pure form  $[\text{ReCH}=\text{CHCH}_3/\text{ReCH}_2\text{CH}=\text{CH}_2; \text{ReCH}=\text{CHCH}(\text{CH}_3)_2/\text{ReCH}_2\text{CH}=\text{C}(\text{CH}_3)_2]$  and show no tendency to interconvert<sup>7b,9,18</sup>. Also, cycloalkene complexes **6b–d** and  $t\text{BuO}^- \text{K}^+$  reacted to give mixtures of vinyl and allyl complexes (vide infra).

It should be emphasized that in the absence of authentic samples of corresponding rhenium vinyl and allyl complexes, structural assignments must be made with caution. For example, under comparable conditions allyl complexes exhibit  $\text{PPh}_3$  ligand  $^{31}\text{P}$ -NMR resonances that are only 2–4 ppm downfield from the corresponding vinyl complexes. A similarly small 0.02–0.10 ppm downfield shift is observed in the cyclopentadienyl  $^1\text{H}$ -NMR resonances. The IR  $\nu_{\text{NO}}$  are  $8\text{--}15 \text{ cm}^{-1}$  greater in vinyl complexes. Thus, a chemical assay of structure was also sought.

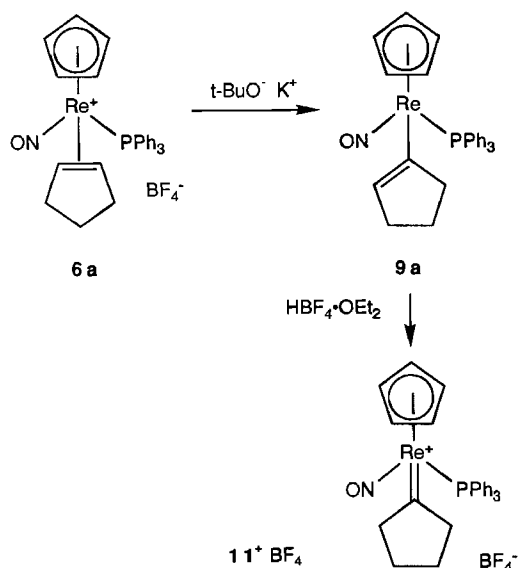
#### 5. Synthesis and Properties of a Cyclopentylidene Complex

Alkylidene complexes  $[(\eta^5\text{-C}_5\text{H}_5)\text{Re}(\text{NO})(\text{PPh}_3)(=\text{CH}-\text{CH}_2\text{R})]^+ \text{X}^-$  also react with mild bases to give vinyl complexes  $(\eta^5\text{-C}_5\text{H}_5)\text{Re}(\text{NO})(\text{PPh}_3)(\text{CH}=\text{CHR})$ <sup>18</sup>. We therefore considered the possibility that cyclopentene complex **6a** might be in rapid equilibrium with a small amount of cyclopentylidene complex  $[(\eta^5\text{-C}_5\text{H}_5)\text{Re}(\text{NO})(\text{PPh}_3)(=\text{C}(\text{CH}_2)_4)]^+ \text{BF}_4^-$  (**11**<sup>+</sup>  $\text{BF}_4^-$ ), which would then be the reactive species towards base. The microscopic reverse of this hydride shift has been observed, but generally at elevated temperatures<sup>19</sup>.

Vinyl complexes  $(\eta^5\text{-C}_5\text{H}_5)\text{Re}(\text{NO})(\text{PPh}_3)(\text{CH}=\text{CHR})$  have previously been shown to react with strong acids  $\text{HX}$  to give alkylidene complexes  $[(\eta^5\text{-C}_5\text{H}_5)\text{Re}(\text{NO})(\text{PPh}_3)(=\text{CHCH}_2\text{R})]^+ \text{X}^-$ <sup>16</sup>. In contrast, allyl complexes  $(\eta^5\text{-C}_5\text{H}_5)\text{Re}(\text{NO})(\text{PPh}_3)(\text{CH}_2\text{CH}=\text{CHR})$  add acids to give alkene complexes  $[(\eta^5\text{-C}_5\text{H}_5)\text{Re}(\text{NO})(\text{PPh}_3)(\text{H}_2\text{C}=\text{CHCH}_2\text{R})]^+ \text{X}^-$ <sup>9</sup>. Thus, the reaction of **9a** with acid was expected to provide both a needed alkylidene complex and a chemical confirmation of structure.

Hence, **9a** was treated with  $\text{HBF}_4 \cdot \text{OEt}_2$  (chlorobenzene,  $-45^\circ\text{C}$ ). Workup gave the anticipated cyclopentylidene complex **11**<sup>+</sup>  $\text{BF}_4^-$  (96%, Scheme 6), which was characterized analogously to the other new compounds above (Table 1). Complex **11**<sup>+</sup>  $\text{BF}_4^-$  exhibited a diagnostic downfield  $\text{Re}=\text{C}$   $^{13}\text{C}$ -NMR resonance ( $\delta = 332$ )<sup>20</sup>. Also, two  $=\text{CCH}_2$  and  $=\text{CCH}_2\text{CH}_2$  resonances were observed, consistent with the appreciable  $\text{Re}=\text{C}$  rotational barriers previously ob-

Scheme 6. Vinylic deprotonation of cyclopentene complex **6a**, and synthesis of cyclopentylidene complex **11**<sup>+</sup>  $\text{BF}_4^-$



served in this series of compounds<sup>20</sup>. The  $\text{PPh}_3$   $^{31}\text{P}$ -NMR resonance of  $11^+ \text{BF}_4^-$  ( $\delta = 14.8$ ) was downfield of those of cycloalkene complexes **6** ( $\delta = 6-9$ ), and close to the range observed for monosubstituted alkylidene complexes  $[(\eta^5\text{-C}_5\text{H}_5)\text{Re}(\text{NO})(\text{PPh}_3)(=\text{CHR})]^+ \text{X}^-$  ( $\delta = 17-20$ )<sup>7b,20f</sup>.

A  $\text{CDCl}_3$  solution of  $11^+ \text{BF}_4^-$  was heated to  $110^\circ\text{C}$  in a sealed NMR tube. No coalescence of the cyclopentylidene ligand  $\text{CH}_2$   $^{13}\text{C}$ -NMR resonances was observed. Application of the coalescence formula<sup>21</sup> established a  $\Delta G_{383\text{ K}}^\ddagger$  of  $\geq 19$  kcal/mol for  $\text{Re}=\text{C}$  bond rotation. Although some decomposition of  $11^+ \text{BF}_4^-$  occurred, no appreciable amount of cyclopentene complex **6a** formed. The independent stability of **6a** and  $11^+ \text{BF}_4^-$  with respect to one another at  $0-110^\circ\text{C}$  precludes any pre-equilibrium isomerization of **6a** prior to deprotonation.

Complex  $11^+ \text{BF}_4^-$  is the first disubstituted alkylidene complex of the  $[(\eta^5\text{-C}_5\text{H}_5)\text{Re}(\text{NO})(\text{PPh}_3)]^+$  fragment to be accessed. Thus, a crystal structure analysis of the hexafluorophosphate salt  $11^+ \text{PF}_6^-$  was executed. Data are summarized in Tables 2–4 and Figure 2. All cyclopentylidene ligand hydrogens were located.

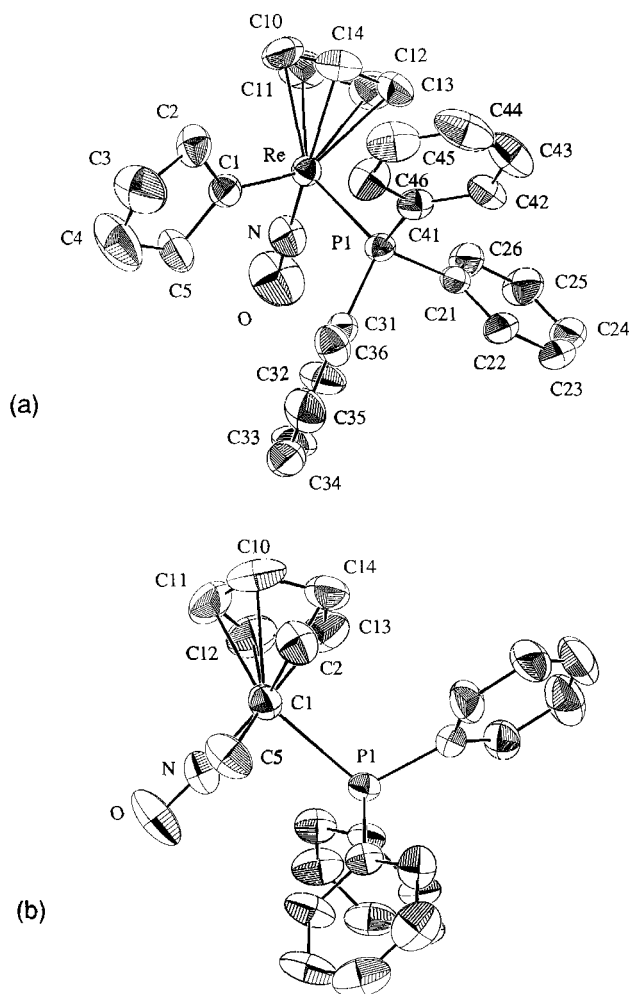


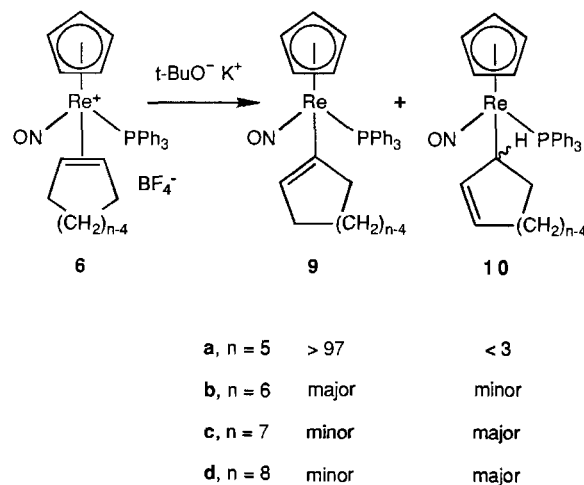
Figure 2. Structure of the cation of cyclopentylidene complex  $[(\eta^5\text{-C}_5\text{H}_5)\text{Re}(\text{NO})(\text{PPh}_3)(=\text{C}(\text{CH}_2)_4)]^+ \text{PF}_6^-$  ( $11^+ \text{PF}_6^-$ ). (a) Numbering diagram; (b) Newman-type projection with C3 and C4 omitted

In order to aid analysis of the  $\text{Re}=\text{C}$  conformation (below), the  $\text{Re}=\text{C}(\text{C})(\text{C}')$  ( $\text{Re}/\text{C}1/\text{C}2/\text{C}5$ ) least-squares plane was calculated. The  $\text{P}-\text{Re}$  and  $\text{N}-\text{Re}$  bonds were found to make  $80.0$  and  $10.5^\circ$  angles with this plane, respectively. The corresponding  $\text{P}-\text{Re}-\text{C}1-\text{C}5$  and  $\text{N}-\text{Re}-\text{C}1-\text{C}5$  torsion angles were similar (Table 4) and differed by ca.  $180^\circ$  from the  $\text{P}-\text{Re}-\text{C}1-\text{C}2$  and  $\text{N}-\text{Re}-\text{C}1-\text{C}2$  torsion angles.

## 6. Other Deprotonation Reactions

THF suspensions of the higher cycloalkene complexes **6b–d** were treated with  $t\text{BuO}^- \text{K}^+$ . Reactions were monitored by  $^{31}\text{P}$  NMR, and product ratios were assayed by peak areas. Cyclohexene complex **6b** gave several products, the two principal components of which exhibited  $^{31}\text{P}$ -NMR resonances at  $\delta = 23.1$  (ca. 45% of total area) and  $24.1$  (19%). The former was assigned to vinyl complex **9b** (Scheme 7), as supported by reactivity data given below.

Scheme 7. Summary of products from the reactions of cycloalkene complexes **6** and  $t\text{BuO}^- \text{K}^+$  in THF



Cycloheptene complex **6c** cleanly gave a ca. 65:35 mixture of two products with  $^{31}\text{P}$ -NMR resonances at  $\delta = 23.1$  and  $22.8$ . Based upon reactivity data given below, these were assigned to two diastereomers of allyl complex **10c** (Scheme 7). Cyclooctene complex **6d** gave two principal products with  $^{31}\text{P}$ -NMR resonances at  $\delta = 20.6$  and  $25.4$  (ca. 20:80). These were assigned to vinyl complex **9d** and allyl complex **10d**, respectively.

These structural assignments were checked by the reactivity test described above for vinyl and allyl complexes. First, reactions were repeated in the mixed solvent  $\text{CH}_2\text{Cl}_2/\text{THF}$  (ca. 2:1 v/v). Under these conditions, product ratios change slightly, but cationic complexes are soluble. Then  $\text{HBF}_4 \cdot \text{OEt}_2$  was added to generate mixtures of cycloalkene and cycloalkylidene complexes. With cyclohexene complex **6b**, the  $^{31}\text{P}$ -NMR resonance that was assigned to vinyl complex **9b** ( $\delta = 22.7$ ,  $\text{CH}_2\text{Cl}_2/\text{THF}$ ) converted to a resonance with a plausible chemical shift for a cyclohexylidene complex ( $\delta = 14.4$ ). A lesser amount of **6b** also reformed ( $\delta = 8.6$ ;

77:23 area ratio). With cycloheptene complex **6c**, analogous deprotonation/reprotonation gave principally **6c** ( $\delta = 6.1$ ). The deprotonation step was not as clean as in THF. However, no  $^{31}\text{P}$ -NMR resonances were found outside of the alkene complex region ( $\delta = 5-10$ ) after  $\text{HBF}_4 \cdot \text{OEt}_2$  addition. With cyclooctene complex **6d**, the resonance that was assigned to allyl complex **10d** ( $\delta = 25.0$ ,  $\text{CH}_2\text{Cl}_2/\text{THF}$ ) converted to **6d** ( $\delta = 9.2$ ).

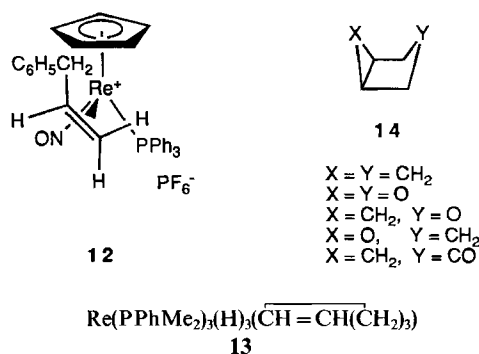
Finally, cyclopentene complexes **6a** and **8** both underwent clean vinylic deprotonation in  $\text{CH}_2\text{Cl}_2/\text{THF}$ , as assayed by  $^{31}\text{P}$ -NMR resonances at  $\delta = 21.2$  and  $23.2$ . The vinyl complex derived from **8** was treated with  $\text{HBF}_4 \cdot \text{OEt}_2$ . A cyclopentylidene complex formed in quantitative yield, as assayed by a  $^{31}\text{P}$ -NMR resonance at  $\delta = 16.9$ . Thus, **6a** and **8** react with  $t\text{BuO}^- \text{K}^+$  in an identical manner. It was similarly verified that cyclopentylidene complex **11** +  $\text{BF}_4^-$  and  $t\text{BuO}^- \text{K}^+$  cleanly react to give vinyl complex **9a**.

## Discussion

### 1. Synthesis and Structure of Cycloalkene Complexes

The cycloalkenes utilized in this study are somewhat less nucleophilic than monosubstituted alkenes towards dichloromethane complex **2** and chlorobenzene complex **3**. Thus **2**, which undergoes an independent and irreversible carbon-chlorine bond cleavage above  $-20^\circ\text{C}$ <sup>21</sup>, generally gives lower yields of complexes than **3**. Other examples where **3** serves as a preparatively superior reagent have been found<sup>3,13</sup>. In work in progress, Scheme 3 has been extended to 3-substituted and 3,4-disubstituted cyclopentene complexes as well as optically active complexes<sup>22</sup>.

Cyclopentene complex **8** shows an overall structure quite similar to that previously found for allylbenzene complex  $(RR,SS)-[(\eta^5\text{-C}_5\text{H}_5)\text{Re}(\text{NO})(\text{PPh}_3)(\text{H}_2\text{C}=\text{CHCH}_2\text{C}_6\text{H}_5)]^+ \text{PF}_6^-$  (**12**)<sup>4</sup>. However, the  $\text{C}\cdots\text{C}$  bond in **8** [1.48(1) Å] is longer than that in **12** [1.398(26) Å]. Cyclopentene and cyclopentane exhibit  $\text{C}=\text{C}$  and  $\text{C}-\text{C}$  bond lengths of 1.343(10) and 1.546(1) Å, respectively<sup>23,24</sup>. Thus, **8** possesses considerable "metallacyclopropane" character.



Curiously, the cyclopentadienyl methyl group is positioned over the cyclopentene ligand in **8** (Figure 1). Since rotational barriers about metal-cyclopentadienyl bonds are low<sup>25</sup>, other cyclopentadienyl ligand conformations should be readily accessible in solution. Thus, the adventitious position of the methyl group in crystalline **8** should

have little bearing on the equilibrium between rotamer types **VI** and **VII** in solution.

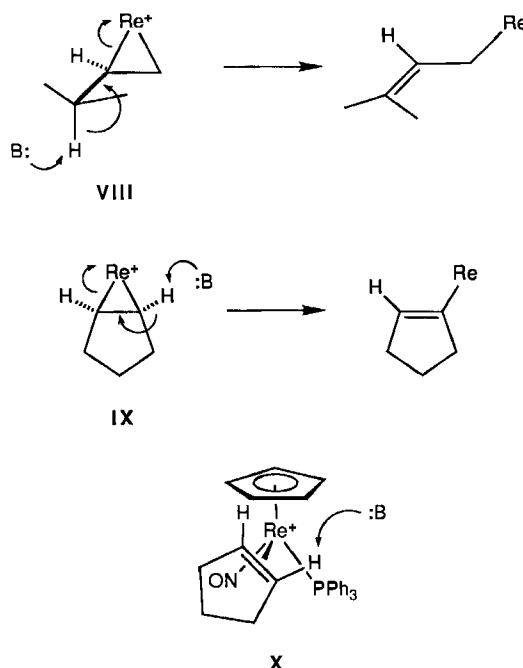
The crystal structure of another rhenium cyclopentene complex,  $\text{Re}(\text{PPhMe}_2)_3(\text{H})_3(\overline{\text{CH}}=\text{CH}(\text{CH}_2)_3)$  (**13**), has been previously described by Caulton<sup>26</sup>. Complex **13** exhibits a  $\text{C}\cdots\text{C}$  bond length [1.423(18) Å] that is slightly shorter than that in **8**. However, the cyclopentene  $\text{Re}-\text{C}$  distances [2.275(14), 2.267(13) Å] are close to those of **8** [2.254(9), 2.257(8) Å].

Structural analogies are frequently drawn between alkene complexes and the corresponding cyclopropanes. Accordingly, the conformational properties of a variety of bicyclo[3.1.0]hexanes of general formula **14** have been studied in detail<sup>27,28</sup>. All exhibit a ground-state "boat" conformation in which the three-membered ring is *syn* to the distal atom of the five-membered ring. Interestingly, the cyclopentene ligand in **8** adopts an analogous conformation, as is best illustrated in Figure 1c. A similar deformation is evident in the crystal structure of cyclopentene complex **13**. Thus, this structural feature appears to have considerable generality.

### 2. Reactivity of Alkene Complexes

The allylic deprotonation of cationic metal alkene complexes has been shown to be an *anti* elimination, as illustrated in transition state **VIII** in Scheme 8<sup>9</sup>. Based upon the hydrogen atom locations depicted in Figure 1c, **8** and by inference **6a** appear to meet the stereoelectronic requirements associated with allylic deprotonation. Thus, the kinetic preference for vinylic deprotonation is surprising and to our knowledge without precedent.

Scheme 8. Some possible transition states for allylic and vinylic deprotonation of alkene complexes



In particular, Rosenblum has reported that iron cyclopentene and cyclohexene complexes of the formula  $[(\eta^5\text{-$

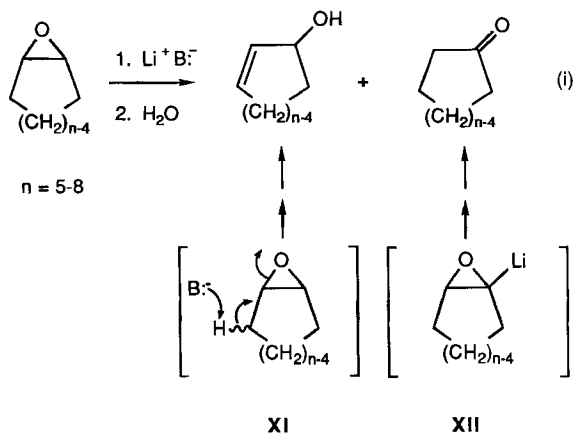
$C_5H_5Fe(CO)_2[\overline{CH=CH(CH_2)_{n-2}}]^+ X^-$  are quantitatively deprotonated by  $Et_3N$  to form the corresponding allyl complexes<sup>8c</sup>. However, an identical reaction of the corresponding cycloheptene complex failed to give an allyl complex. In contrast, we observe an increasing tendency for allylic deprotonation in this series. Amine bases are generally too weak to deprotonate rhenium alkene complexes<sup>9</sup>. Thus, we are unable to determine product distributions under conditions analogous to Rosenblum's.

Varying amounts of vinylic deprotonation have also been observed with monosubstituted alkene complexes  $[(\eta^5-C_5H_5)Re(NO)(PPh_3)(RCH=CH_2)]^+ X^-$  (**5**)<sup>7b</sup>. Only vinylic deprotonation is observed when R is a bulky isopropyl group. Allylic deprotonation usually dominates when R is a small methyl group. This trend will be fully analyzed in a subsequent full paper<sup>29</sup>. However, transition state **VIII** should become energetically less accessible as the allylic carbon bears increasing numbers of substituents.

Deuterium labeling studies with monosubstituted alkene complexes **5** have confirmed that the proton is abstracted from a vinylic position<sup>7b</sup>, as opposed to an allylic position followed by rearrangement. The rhenium assumes the position of the abstracted proton, as shown in **IX** (Scheme 8). Also, regardless of the diastereomer of **5** employed, the proton abstracted always corresponds to that shown in **X**. Unfortunately, no means presently exists for stereospecifically labeling one of the two vinylic protons in **6a** with deuterium, or probing whether **X** is preferred over a transition state involving a type **VII** rotamer.

Reactions of epoxides of cycloalkenes with strong lithium dialkylamide and lithium alkyl bases have been studied in detail<sup>30a</sup> and provide some analogy for the data in Scheme 7. As shown in equation (i), varying mixtures of two products are commonly obtained. The dominant product is usually an allylic alcohol, which forms by an elimination **XI** that is obviously related to **VIII** in Scheme 8. However, appreciable amounts of ketones are also produced. These are believed to form by the initial lithiation of the epoxide ring (**XII**), a pathway that is related to **IX** in Scheme 8. The product distributions are very dependent upon the substrate, base, and reaction conditions<sup>30b</sup>.

In free cycloalkenes, the allylic protons are thermodynamically more acidic than the vinylic protons ( $pK_{C_8CHA} =$



44–46)<sup>31</sup>. We have to date been unable to establish whether allylic or vinylic deprotonation is thermodynamically preferred with the rhenium complexes<sup>7b</sup>. The reactivity order cycloheptene > cyclooctene  $\approx$  cyclohexene > cyclopentene has been found for allylic proton exchange with  $Li^+ RND^- / RND_2$ . A detailed analysis showed that no simple model accounts for this trend<sup>31</sup>. However, the data parallel the allyl/vinyl selectivities in Scheme 7.

### 3. Properties of Cyclopentylidene Complexes

The structure of cyclopentylidene complex **11**<sup>+</sup>  $PF_6^-$  (Figure 2) shows many similarities to that of benzylidene complex  $[(\eta^5-C_5H_5)Re(NO)(PPh_3)(=CHC_6H_5)]^+ PF_6^-$  (**15**; Figure 3)<sup>18a</sup>. First, the Re=C bond lengths are identical [1.945(4), 1.949(6) Å]. Second, both compounds exhibit Re=C conformations that maximize overlap of the d donor orbital shown in **I** with the  $C_\alpha$  p acceptor orbital<sup>18a</sup>.

$[(\eta^5-C_5H_5)Re(NO)(PPh_3)(=CHC_6H_5)]^+ PF_6^-$   
**15**

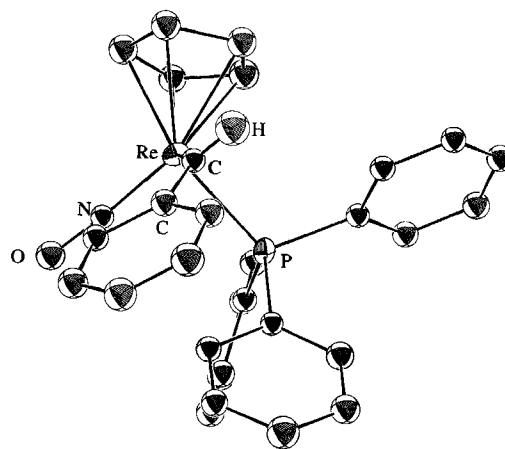


Figure 3. Structure of the cation of benzylidene complex  $[(\eta^5-C_5H_5)Re(NO)(PPh_3)(=CHC_6H_5)]^+ PF_6^-$  (**15**)

The Re=C conformations can be compared in several ways. First, the P–Re–C–C and N–Re–C–C torsion angles in **15** are  $-88$  and  $4^\circ$ , respectively, as opposed to  $-84$  and  $8^\circ$  for the P1–Re–C1–C5 and N–Re–C1–C5 torsion angles in **11**<sup>+</sup>  $PF_6^-$  (Table 4). Also, the Re=C(H)(C) least-squares plane of **15** can be calculated. The Re–P and Re–N bonds make angles of  $87$  and  $3^\circ$  with this plane, respectively. The corresponding angles involving the Re=C(C)(C') least squares plane of **11**<sup>+</sup>  $PF_6^-$  are  $80.0$  and  $10.5^\circ$ .

The Re=C–C angles in **11**<sup>+</sup>  $PF_6^-$  [ $128.3(3)$ ,  $127.0(3)^\circ$ ] are greater than the C–C $_\alpha$ –C angle [ $104.6(3)^\circ$ ]. An analogous deformation has been found in cyclopentanone [C–C(O)–C,  $108.6(2)^\circ$ ]<sup>32</sup>. Interestingly, the crystal structures of several tungsten(IV) cyclopentylidene complexes have been described by Mayer<sup>33</sup> and Osborn<sup>34</sup>. These include  $W(O)Cl_2(PMePh_2)(=C(CH_2)_4)$  and two complexes of the formula  $W(OR)_2(X)_3(=C(CH_2)_4)$  (X = Br or bridging

Br). Their W=C bond lengths are 1.980(12), 1.890(5), and 1.896(9) Å, respectively.

#### 4. Summary

This study has established the ready availability of cycloalkene complexes of the chiral rhenium fragment **1**. Interestingly, these complexes undergo either vinylic or allylic deprotonation by the mild base  $t\text{BuO}^- \text{K}^+$ . The dominant pathway is a sensitive function of substrate and reaction conditions. Some diastereoselectivity (Scheme 2) appears to attend the allylic deprotonation of **6d**. However, vinylic deprotonation allows access to heretofore inaccessible cycloalkylidene complexes.

The above data hint that cationic metal alkene complexes might exhibit a wealth of unanticipated carbon-hydrogen bond activation reactions. Future reports will extend this study to adducts of **1** and acyclic *cis*- and *trans*-disubstituted alkenes.

We thank the *National Institutes of Health* and the *Department of Energy* for support of this research, and the *National Institutes of Health* for a postdoctoral fellowship (J.J.K.).

#### Experimental

General procedures (instrumentation, analytical/mp data, dynamic and NOE-NMR experiments, solvent purifications) were identical to those given in a recent paper<sup>12</sup>. Reagents were treated as follows: Cycloalkenes (Aldrich), filtered through alumina ( $\text{C}_3$ ) or distilled from Na ( $\text{C}_6$ – $\text{C}_8$ );  $t\text{BuO}^- \text{K}^+$  in THF,  $\text{NH}_4^+ \text{PF}_6^-$  (Aldrich),  $\text{CH}_3\text{I}$  (Fisher), used as received;  $n\text{BuLi}$  (Aldrich), standardized before use<sup>35</sup>.

$[(\eta^5\text{-C}_5\text{H}_5)\text{Re}(\text{NO})(\text{PPh}_3)(\overline{\text{CH}=\text{CH}(\text{CH}_2)_3})]^+ \text{BF}_4^-$  (**6a**): A Schlenk flask was charged with  $(\eta^5\text{-C}_5\text{H}_5)\text{Re}(\text{NO})(\text{PPh}_3)(\text{CH}_3)$  (**1**; 0.469 g, 0.839 mmol)<sup>36</sup>, chlorobenzene (10 ml), and a stir bar, capped with a septum, and cooled to  $-45^\circ\text{C}$  (acetonitrile/liquid  $\text{N}_2$  slurry). Then  $\text{HBF}_4 \cdot \text{OEt}_2$  (0.135 ml, 0.843 mmol) was added with stirring. After 10 min, cyclopentene (0.740 ml, 5.837 mmol) was added. The reaction mixture was allowed to slowly warm to room temp. over ca. 3 h, and was stirred overnight. Some powder precipitated. The brown suspension was added dropwise to rapidly stirred ether (75 ml, in air). The reaction flask was rinsed with  $\text{CH}_2\text{Cl}_2$  (1–2 ml), which was added to the ether. The resulting precipitate was collected by filtration, washed with ether, and dried under oil pump vacuum ( $56^\circ\text{C}$ ) to give **6a** as a light tan powder (0.552 g, 0.790 mmol, 94%), mp  $190$ – $192^\circ\text{C}$  (dec.).

$\text{C}_{28}\text{H}_{28}\text{BF}_4\text{NOPRe}$  (698.5) Calcd. C 48.15 H 4.04  
Found C 48.00 H 4.06

A sample was crystallized from layered  $\text{CH}_2\text{Cl}_2$ /hexane. This gave **6a** as amber slivers, which were dried under oil pump vacuum ( $56^\circ\text{C}$ ), mp  $193$ – $194^\circ\text{C}$  (dec.).

Found C 47.89 H 4.01

$[(\eta^5\text{-C}_5\text{H}_5)\text{Re}(\text{NO})(\text{PPh}_3)(\overline{\text{CH}=\text{CH}(\text{CH}_2)_4})]^+ \text{BF}_4^-$  (**6b**): Complex **1** (0.203 g, 0.364 mmol), chlorobenzene (4 ml),  $\text{HBF}_4 \cdot \text{OEt}_2$  (0.060 ml, 0.38 mmol), and cyclohexene (0.150 ml, 1.48 mmol) were combined in a procedure analogous to that given for **6a**. An identical workup gave **6a** as a light tan powder (0.230 g, 0.323 mmol, 89%), mp  $114$ – $116^\circ\text{C}$  (dec.).

$\text{C}_{29}\text{H}_{30}\text{BF}_4\text{NOPRe}$  (712.5) Calcd. C 48.88 H 4.24  
Found C 48.95 H 4.19

$[(\eta^5\text{-C}_5\text{H}_5)\text{Re}(\text{NO})(\text{PPh}_3)(\overline{\text{CH}=\text{CH}(\text{CH}_2)_5})]^+ \text{BF}_4^-$  (**6c**): Complex **1** (0.144 g, 0.257 mmol), chlorobenzene (3.5 ml),  $\text{HBF}_4 \cdot \text{OEt}_2$  (0.041 ml, 0.26 mmol), and cycloheptene (0.120 ml, 1.03 mmol) were combined in a procedure analogous to that given for **6a**. An identical workup gave **6c** as a light brown powder (0.148 g, 0.203 mmol, 79%) that was nearly analytically pure. A sample (0.132 g, 0.181 mmol) was flash-chromatographed on silica (230–400 mesh, 10% acetone/ $\text{CH}_2\text{Cl}_2$ ) and dried under oil pump vacuum ( $56^\circ\text{C}$ ) to give **6c** as a golden powder (0.085 g, 0.118 mmol, 65%), mp  $118$ – $122^\circ\text{C}$  (dec.).

$\text{C}_{30}\text{H}_{32}\text{BF}_4\text{NOPRe}$  (726.6) Calcd. C 49.59 H 4.44  
Found C 49.51 H 4.44

$[(\eta^5\text{-C}_5\text{H}_5)\text{Re}(\text{NO})(\text{PPh}_3)(\overline{\text{CH}=\text{CH}(\text{CH}_2)_6})]^+ \text{BF}_4^-$  (**6d**): Complex **1** (0.209 g, 0.374 mmol), chlorobenzene (4 ml),  $\text{HBF}_4 \cdot \text{OEt}_2$  (0.060 ml, 0.38 mmol), and *cis*-cyclooctene (0.195 ml, 1.50 mmol) were combined in a procedure analogous to that given for **6a**. An identical workup gave **6d** as a light tan powder (0.243 g, 0.328 mmol, 88%), mp  $203$ – $205^\circ\text{C}$  (dec.).

$\text{C}_{31}\text{H}_{34}\text{BF}_4\text{NOPRe}$  (740.6) Calcd. C 50.28 H 4.63  
Found C 50.35 H 4.66

$(\eta^5\text{-C}_5\text{H}_4\text{CH}_3)\text{Re}(\text{NO})(\text{PPh}_3)(\text{CH}_3)$  (**7**): A Schlenk flask was charged with **1** (0.560 g, 1.00 mmol), THF (30 ml), and a stir bar, capped with a septum, and cooled to  $-29^\circ\text{C}$  ( $\text{CH}_3\text{NO}_2$ /liquid  $\text{N}_2$  slurry). Then  $n\text{BuLi}$  (0.850 ml, 2.36 M in hexane) was added. The solution was stirred for 5.5 h, and then  $\text{CH}_3\text{I}$  (0.135 ml, 2.11 mmol) was added. The orange solution was allowed to slowly warm to room temp. over 12 h, and was then filtered through layered silica/Celite (1.5 cm/1.5 cm) with several THF rinses. The filtrate was concentrated to a red-orange oil by rotary evaporation. The oil was dissolved in benzene (ca. 25 ml) and filtered through silica/Celite (with benzene rinses) as above. Heptane (10 ml) was added to the filtrate. Solvents were removed by rotary evaporation to give **7** as a bright orange powder that was dried under oil pump vacuum (0.470 g, 0.820 mmol, 82%), mp  $148$ – $151^\circ\text{C}$ .

$\text{C}_{25}\text{H}_{25}\text{NOPRe}$  (572.7) Calcd. C 52.44 H 4.40  
Found C 52.72 H 4.42

$[(\eta^5\text{-C}_5\text{H}_4\text{CH}_3)\text{Re}(\text{NO})(\text{PPh}_3)(\overline{\text{CH}=\text{CH}(\text{CH}_2)_3})]^+ \text{BF}_4^-$  (**8**): Complex **7** (0.134 g, 0.235 mmol), chlorobenzene (4 ml),  $\text{HBF}_4 \cdot \text{OEt}_2$  (0.040 ml, 0.25 mmol), and cyclopentene (0.150 ml, 1.48 mmol) were combined in a procedure analogous to that given for **6a**. An identical workup gave **8** as a dull yellow powder (0.147 g, 0.206 mmol, 88%), mp  $180$ – $183^\circ\text{C}$  (dec.).

$\text{C}_{29}\text{H}_{30}\text{BF}_4\text{NOPRe}$  (712.5) Calcd. C 48.88 H 4.24  
Found C 48.82 H 4.22

A sample was crystallized from layered  $\text{CH}_2\text{Cl}_2$ /pentane. This gave **8** as amber trigonal plates, which were dried under a  $\text{N}_2$  stream, mp  $185$ – $187^\circ\text{C}$  (dec.). Density (floatation,  $\text{CCl}_4/\text{CH}_2\text{I}_2$ ): 1.68 g/ml.

Found C 48.65 H 4.15

$(\eta^5\text{-C}_5\text{H}_5)\text{Re}(\text{NO})(\text{PPh}_3)(\overline{\text{C}=\text{CH}(\text{CH}_2)_3})$  (**9a**): A Schlenk flask was charged with **6a** (0.178 g, 0.255 mmol), THF (5 ml), and a stir bar, capped with a septum, and cooled to  $-80^\circ\text{C}$  (acetone/dry ice). Then  $t\text{BuO}^- \text{K}^+$  (0.300 ml, 1.0 M in THF) was added to the suspension with stirring. The bath was allowed to slowly warm to room temp. over 3 h. Solvent was removed under oil pump vacuum, and the orange-red residue was extracted with  $\text{CH}_2\text{Cl}_2$  ( $3 \times 2$  ml). The extracts were sequentially transferred by a cannula to a Kramer filter containing a  $1 \times 3$  cm column of base-treated Florisil (10 ml concentrated aqueous  $\text{NH}_3/35$  g Florisil). The filtrates were collected in a tared flask and concentrated to ca. 2 ml under oil pump vacuum. Then hexane (4 ml) was added, and a precipitate formed. Solvents were removed under oil pump vacuum

(15 h) to give **9a** as a red-orange powder (0.140 g, 0.228 mmol, 90%), dec. p. ca. 112 °C (darkening, mp > 210 °C).

$C_{28}H_{27}NOPRe$  (610.7) Calcd. C 55.07 H 4.46  
Found C 55.22 H 4.55

$[(\eta^5-C_5H_5)Re(NO)(PPh_3)(=\bar{C}(\bar{C}H_2)_4)]^+ BF_4^-$  (**11**<sup>+</sup>  $BF_4^-$ ): A Schlenk flask was charged with **9a** (0.106 g, 0.174 mmol), chlorobenzene (3 ml), and a stir bar, capped with a septum, and cooled to -45 °C (acetonitrile/liquid N<sub>2</sub> slurry). Then HBF<sub>4</sub> · OEt<sub>2</sub> (0.030 ml, 0.187 mmol) was added with stirring. The solution was allowed to slowly warm to room temp. over ca. 5 h. Some precipitate formed. The suspension was transferred dropwise (with a 1–2-ml chlorobenzene rinse) to rapidly stirred hexane (20 ml, by a cannula under N<sub>2</sub>). The resulting precipitate was collected by filtration, washed with hexane and pentane, and dried under oil pump vacuum (48 h, room temp.) to give **11**<sup>+</sup>  $BF_4^-$  as a dull grey-brown powder (0.116 g, 0.166 mmol, 96%), mp 127–132 °C (dec.).

$C_{28}H_{28}BF_4NOPRe$  (698.5) Calcd. C 48.15 H 4.04  
Found C 48.09 H 4.06

$[(\eta^5-C_5H_5)Re(NO)(PPh_3)(=\bar{C}(\bar{C}H_2)_4)]^+ PF_6^-$  (**11**<sup>+</sup>  $PF_6^-$ ): A flask was charged with **11**<sup>+</sup>  $BF_4^-$  (0.055 g, 0.079 mmol), NH<sub>4</sub><sup>+</sup>  $PF_6^-$  (0.131 g, 0.804 mmol), acetone (8 ml), and a stir bar and was fitted with an N<sub>2</sub> inlet. The resulting solution was stirred for 4 h. Solvent was removed by rotary evaporation, and the light brown residue was extracted with CHCl<sub>3</sub> (5 × 2 ml). The combined extracts were filtered, and the solvent was removed from the filtrate by rotary evaporation. The residue was extracted with CHCl<sub>3</sub> (3 ml). The extract was filtered and the filtrate added dropwise to rapidly stirred hexane (25 ml). The resulting precipitate was collected by filtration, washed with pentane, and dried under oil pump vacuum (56 °C) to give **11**<sup>+</sup>  $PF_6^-$  as an off-white powder (0.046 g, 0.061 mmol, 77%), mp 104–107 °C (dec.).

$C_{28}H_{28}F_6NOP_2Re$  (756.7) Calcd. C 44.45 H 3.73  
Found C 44.46 H 3.77

A sample was crystallized from layered CH<sub>2</sub>Cl<sub>2</sub>/pentane. This gave **11**<sup>+</sup>  $PF_6^-$  as amber irregularly shaped crystals (including large plates), which were dried under an N<sub>2</sub> stream, mp 135–137 °C (dec.). Density (flotation, CCl<sub>4</sub>/CH<sub>2</sub>I<sub>2</sub>): 1.77 g/ml.

Found C 44.34 H 3.72

**X-ray Crystal Structures**<sup>37</sup>: An amber cube of **8**, obtained as described above, was mounted for data collection on a Syntex PI automated diffractometer as summarized in Table 2. Cell constants were determined from 30 centered reflections with 20° < 2Θ < 30°. The space group was determined from systematic absences (*h*0*l* *h* = 2*n*, 0*kl* *k* + *l* = 2*n*, *h*00 *h* = 2*n*, 0*kl* *k* = 2*n*, 00*l* *l* = 2*n*) and subsequent least-squares refinement. Lorentz, polarization, and empirical absorption corrections were applied. The structure was solved by standard heavy-atom techniques with the SDP/VAX package<sup>38</sup>. Hydrogen atoms H1–H8 were located from the final Fourier difference map. Other hydrogen atom positions were calculated. All hydrogen atom positions were included in the structure factor calculations. Non-hydrogen atoms were refined with anisotropic thermal parameters. Anomalous dispersion corrections were applied throughout the refinement. Scattering factors, and Δ*f*' and Δ*f*" values were taken from the literature<sup>39</sup>.

An amber plate of **11**<sup>+</sup>  $PF_6^-$ , obtained as described above, was mounted for data collection on a CAD 4 automated diffractometer as summarized in Table 2. The structure determination, which included the location of the cyclopentylidene ligand hydrogen atoms (H1–H8) from a difference map, was conducted analogously to **8**.

## CAS Registry Numbers

1: 71763-18-3 / **6a**: 131214-68-1 / **6b**: 131214-70-5 / **6c**: 131214-72-7 / **6d**: 131214-74-9 / **7**: 131214-75-0 / **8**: 131214-77-2 / **9a**: 131214-78-3 / **9b**: 131214-82-9 / **10c**: 131214-83-0 / **10d**: 131235-88-6 / **11** · BF<sub>4</sub>: 131214-80-7 / **11** · PF<sub>6</sub>: 131214-81-8 / cyclopentene: 142-29-0 / cyclohexene: 110-83-8 / cycloheptene: 628-92-2 / *cis*-cyclooctene: 931-87-3

- <sup>1</sup> Some lead references: <sup>1a)</sup> C.-K. Chou, D. L. Miles, R. Bau, T. C. Flood, *J. Am. Chem. Soc.* **100** (1978) 7271. — <sup>1b)</sup> J. W. Faller, K.-H. Chao, *Organometallics* **3** (1984) 927. — <sup>1c)</sup> G. Consiglio, F. Morandini, *Chem. Rev.* **87** (1987) 761.
- <sup>2</sup> J. M. Fernández, J. A. Gladysz, *Organometallics* **8** (1989) 207.
- <sup>3</sup> J. J. Kowalczyk, S. K. Agbassou, J. A. Gladysz, *J. Organomet. Chem.* **384** (1990), 333.
- <sup>4</sup> G. S. Bodner, T.-S. Peng, A. M. Arif, J. A. Gladysz, *Organometallics* **9** (1990) 1191.
- <sup>5</sup> R/S nomenclature conventions are described in ref.<sup>4</sup>.
- <sup>6</sup> T.-S. Peng, J. A. Gladysz, *Tetrahedron Lett.* **31** (1990) 4417.
- <sup>7a)</sup> T.-S. Peng, J. A. Gladysz, *J. Chem. Soc., Chem. Commun.* **1990**, 902. — <sup>7b)</sup> T.-S. Peng, J. A. Gladysz, *Organometallics* **9** (1990), 2884.
- <sup>8a)</sup> M. Rosenblum, *J. Organomet. Chem.* **300** (1986) 191. — <sup>8b)</sup> A. Cutler, D. Ehntholt, W. P. Giering, P. Lennon, S. Raghu, A. Rosan, M. Rosenblum, J. Tancrede, D. Wells, *J. Am. Chem. Soc.* **98** (1976) 3495. — <sup>8c)</sup> W. P. Giering, S. Raghu, M. Rosenblum, A. Cutler, D. Ehntholt, R. W. Fish, *J. Am. Chem. Soc.* **94** (1972) 8251.
- <sup>9</sup> G. S. Bodner, K. Emerson, R. D. Larsen, J. A. Gladysz, *Organometallics* **8** (1989) 2399.
- <sup>10</sup> P. C. Heah, A. T. Patton, J. A. Gladysz, *J. Am. Chem. Soc.* **108** (1986) 1185.
- <sup>11a)</sup> P. Johnston, M. S. Loonat, W. L. Ingham, L. Carlton, N. J. Coville, *Organometallics* **6** (1987) 2121. — <sup>11b)</sup> L. Carlton, P. Johnston, N. J. Coville, *J. Organomet. Chem.* **339** (1988) 339.
- <sup>12</sup> B. E. Mann, B. F. Taylor, *<sup>13</sup>C NMR Data for Organometallic Compounds*, p. 184–199, Academic Press, New York 1981.
- <sup>13</sup> J. J. Kowalczyk, A. M. Arif, J. A. Gladysz, *Organometallics* **10** (1991), in press.
- <sup>14</sup> H. Günther, *NMR Spectroscopy*, p. 376, Wiley, New York 1980.
- <sup>15</sup> J. W. Fitch, E. B. Ripplinger, B. A. Shoulders, S. D. Sorey, *J. Organomet. Chem.* **352** (1988) C25.
- <sup>16</sup> D. Neuhaus, M. Williamson, *The Nuclear Overhauser Effect in Structural and Conformational Analyses*, chapter 7, VCH Verlagsgesellschaft, New York 1989.
- <sup>17</sup> S. D. Ittel, J. A. Ibers, *Adv. Organomet. Chem.* **14** (1976) 33.
- <sup>18</sup> G. S. Bodner, D. E. Smith, W. G. Hatton, P. C. Heah, S. Georgiou, A. L. Rheingold, S. J. Geib, J. P. Hutchinson, J. A. Gladysz, *J. Am. Chem. Soc.* **109** (1987) 7688.
- <sup>19a)</sup> W. G. Hatton, J. A. Gladysz, *J. Am. Chem. Soc.* **105** (1983) 1846. — <sup>19b)</sup> C. Roger, G. S. Bodner, W. G. Hatton, J. A. Gladysz, manuscript in preparation.
- <sup>20a)</sup> W. A. Kiel, G.-Y. Lin, A. G. Constable, F. B. McCormick, C. E. Strouse, O. Eisenstein, J. A. Gladysz, *J. Am. Chem. Soc.* **104** (1982) 4865. — <sup>20b)</sup> W. A. Kiel, G.-Y. Lin, G. S. Bodner, J. A. Gladysz, *J. Am. Chem. Soc.* **105** (1983) 4958. — <sup>20c)</sup> A. T. Patton, C. E. Strouse, C. B. Knobler, J. A. Gladysz, *J. Am. Chem. Soc.* **105** (1983) 5804. — <sup>20d)</sup> J. H. Merrifield, G.-Y. Lin, W. A. Kiel, J. A. Gladysz, *J. Am. Chem. Soc.* **105** (1983) 5811. — <sup>20e)</sup> W. A. Kiel, W. E. Buhro, J. A. Gladysz, *Organometallics* **3** (1984) 879. — <sup>20f)</sup> E. J. O'Connor, M. Kobayashi, H. G. Floss, J. A. Gladysz, *J. Am. Chem. Soc.* **109** (1987) 4837.
- <sup>21</sup> J. Sandström, *Dynamic NMR Spectroscopy*, chapter 7, Academic Press, New York 1982.
- <sup>22</sup> J. J. Kowalczyk, unpublished results, University of Utah.
- <sup>23a)</sup> G. W. Rathens Jr., *J. Chem. Phys.* **36** (1962) 2401. — <sup>23b)</sup> M. I. Davis, T. W. Muecke, *J. Phys. Chem.* **74** (1970) 1104.
- <sup>24</sup> W. J. Adams, H. J. Geise, L. S. Bartell, *J. Am. Chem. Soc.* **92** (1970) 5013.
- <sup>25</sup> Recent lead references: <sup>25a)</sup> R. Mynott, H. Lehmkuhl, E.-M. Kreuzer, E. Joussen, *Angew. Chem., Int. Ed. Engl.* **29** (1990) 289. — <sup>25b)</sup> M. I. Altbach, Y. Hiyama, R. J. Wittebort, L. G. Bulter, *Inorg. Chem.* **29** (1990) 741.
- <sup>26</sup> M. A. Green, J. C. Huffman, K. G. Caulton, W. K. Rybak, J. J. Ziolkowski, *J. Organomet. Chem.* **218** (1981) C39.
- <sup>27</sup> Review of conformation in cyclopentane, cyclopentene, and bicyclic derivatives: A. C. Legon, *Chem. Rev.* **80** (1980) 231.

- <sup>28)</sup> <sup>28a)</sup> R. C. Lord, T. B. Malloy Jr., *J. Mol. Spect.* **46** (1973) 358. — <sup>28b)</sup> J. D. Lewis, J. Laane, T. B. Malloy Jr., *J. Chem. Phys.* **61** (1974) 2342. — <sup>28c)</sup> R. L. Cook, T. B. Malloy Jr., *J. Am. Chem. Soc.* **96** (1974) 1703. — <sup>28d)</sup> J. W. Bevan, A. C. Legon, S. O. Ljunggren, P. J. Mjöberg, *J. Am. Chem. Soc.* **100** (1978) 8161.
- <sup>29)</sup> T.-S. Peng, J. A. Gladysz, manuscript in preparation.
- <sup>30)</sup> <sup>30a)</sup> J. K. Crandall, M. Appar, *Org. React.* **29** (1983) 345. — <sup>30b)</sup> G. A. Molander, K. Mautner, *J. Org. Chem.* **54** (1989) 4042.
- <sup>31)</sup> A. Streitwieser, Jr., D. W. Boerth, *J. Am. Chem. Soc.* **100** (1978) 755.
- <sup>32)</sup> K. Tamagawa, R. L. Hilderbrandt, Q. Shen, *J. Am. Chem. Soc.* **109** (1987) 1380.
- <sup>33)</sup> J. C. Bryan, J. M. Mayer, *J. Am. Chem. Soc.* **109** (1987) 7213; **112** (1990) 2298.
- <sup>34)</sup> M. T. Youinou, J. Kress, J. Fischer, A. Aguero, J. A. Osborn, *J. Am. Chem. Soc.* **110** (1988) 1488.
- <sup>35)</sup> W. G. Kofron, L. M. Baclawski, *J. Org. Chem.* **41** (1976) 1879.
- <sup>36)</sup> W. Tam, G.-Y. Lin, W.-K. Wong, W. A. Kicel, V. K. Wong, J. A. Gladysz, *J. Am. Chem. Soc.* **104** (1982) 141.
- <sup>37)</sup> Further details and basic data concerning the X-ray analyses may be obtained from Fachinformationszentrum Karlsruhe, Gesellschaft für wissenschaftlich-technische Information, D-7514 Eggenstein-Leopoldshafen (F.R.G.) by specifying registry number CSD-54855, author, and the reference to this publication.
- <sup>38)</sup> B. A. Frenz, in "The Enraf-Nonius CAD 4 SDP — A Real-time System for Concurrent X-ray Data Collection and Crystal Structure Determination", in *Computing and Crystallography* (H. Schenk, R. Olthof-Hazelkamp, H. van Konigsveld, G. C. Bassi, Eds.), p. 64–71, Delft University Press, Delft, Holland 1978.
- <sup>39)</sup> D. T. Cromer, J. T. Waber, in *International Tables for X-ray Crystallography* (J. A. Ibers, W. C. Hamilton, Eds.), vol. IV, p. 72–98, 149–150; tables 2.2B and 2.3.1, Kynoch, Birmingham, England 1974.

[329/90]